17 Mesozoic assembly of Asia: constraints from fossil floras, tectonics, and paleomagnetism

ALFRED M. ZIEGLER, PETER M. REES, DAVID B. ROWLEY, ANDREY BEKKER, LI QING, and MICHAEL L. HULVER

[*In: The Tectonic Evolution of Asia, A. Yin and M. Harrison (eds.), pp. 371-400. Cambridge: Cambridge University Press.* (1996). This is the unformatted text - see publication for pagination]

Abstract

A floral gradient for the early Mesozoic has been reconstructed from localities ranging from the subtropics to the polar region of the Northern Hemisphere, encompassing climates interpreted as having ranged from the warm dry subtropical to the cool wet temperate regime. Our previous ordination studies on the floras had demonstrated a gradual replacement of morphological types: from coniferophytes and cycadophytes with thick cuticles and small leaves in low latitudes, through broader-leaved forms of cycadophytes with filicopsids, to broad-leaved deciduous ginkgophytes and coniferophytes in near-polar positions. Parallels with the Recent tropical and subtropical distributions of the cycads and with the late Cenozoic temperate distribution of *Ginkgo* can be drawn.

Floral lists were assembled from eight exceptionally well sampled regions in Northern Eurasia ranging in age from late Triassic through late Jurassic, and were used to determine the correlation of the floral gradient with paleo-latitude. Floral lists were also assembled from basins associated with the Chinese microcontinents of South China, North China and Tarim, which were converging with Northern Eurasia at the time. Their positions are therefore less well known, and our purpose is to show that the floral gradient is sensitive enough to be used as a check on the tectonic- and paleomagnetic-based reconstructions currently available. South China and North China were in the warm temperate zone in the late Triassic and early Jurassic, and collision with the southward-moving Eurasia was complete by the late Jurassic. During the Jurassic, the complex was moving equatorward into the dry subtropical zone. These conclusions accord with current tectonic interpretations, but the available paleomagnetic data seem to underestimate significantly the paleo-latitude of these blocks during some time intervals.

Introduction

In a recent paper, "Early Mesozoic Phytogeography and Climate," Ziegler et al. (1993) presented reconstructions of Eurasia, showing floral patterns for seven intervals ranging throughout the Triassic and Jurassic. That multivariate analysis of several hundred macrofloral lists represents a first attempt to quantify gradations that have been described and interpreted for many years by Russian authors (Vakhrameev et al., 1978; Krassilov, 1981; Dobruskina, 1982). The localities range in paleo-latitude from about 20°N to 80°N and "can be interpreted climatically as ranging through the dry subtropical to the warm and cool temperate biomes" (Ziegler et al., 1993). Many authors have delineated climate zones using the floras, though it must be admitted that sharp transitions do not exist, and the purpose of this chapter is to explore the character of what is, in reality, a smooth gradient.

Of particular interest are the matters of the latitudinal consistency of the floral gradient through time and whether or not it can be employed to test the predictions of paleomagnetists with respect to the paleo-latitudes of the microcontinental elements of China (Enkin et al., 1992). A number of these elements, including central Mongolia, were closing with Siberia along the Mongol-Okhotsk belt until the end of the Jurassic (Zonenshain Kuzmin, and Napatov, 1990). Our strategy is to determine the correlation of the floral gradient with paleo-latitude from the localities associated with northern Eurasia. This vast region was an integral part of Pangaea until the mid-Jurassic, so its orientation is relatively well known, and it provides a model against which the floras of China may be compared. Fortunately, there was free geographic interchange between areas, to judge by current paleogeographic reconstructions and the continuity of the floras. Also, the floras were remarkably stable during the "Mesophytic" (Meyen, 1987), the long interval spanning the Late Triassic, the Jurassic, and the early Cretaceous; see Spicer, Rees, and Chapman (1993) for Cretaceous floral maps.

Paleontologists may be surprised by these claims of geographic and temporal continuity, but they are supported by an equally remarkable fossil record in continental deposits that has been documented from thousands of sites for each interval by European, Russian and Chinese paleobotanists. The absence of geographic barriers is perhaps not surprising during Pangaean intervals. In this connection, the Permian phytogeography is similar to the early Mesozoic in that all the floral provinces can be accounted for by climate in terms

of variations in the patterns of precipitation and temperature (Ziegler, 1990). The temporal continuity is partly artifactual, in that the preservation in many cases is insufficient for precise identifications; so many of the taxa are "form-genera." Our experience is that the form in general reflects the climate. There can be no doubt, however, that a condition of climatic and evolutionary stasis existed in Eurasia throughout much of the Mesozoic. Certain climate changes that have been described (Hallam, 1993) were, in our view, the effects of the continent moving with respect to the climate zones, rather than the reverse (Ziegler et al., 1993).

Floral-gradient determination

Our multivariate statistical analysis of seven Triassic and Jurassic temporal intervals demonstrated a correlation of floral variation with paleolatitude as reconstructed from paleomagnetic and tectonic information (Ziegler et al., 1993). A matrix was constructed for each interval from taxonomic lists assembled from localities throughout Eurasia and submitted to a computer ordination program called Decorana (Gauch, 1982). "Geometrically, ordination involves rotation and transformation of the original multidimensional coordinate system and reduction of high dimensionality so that major directions of variation within the data set can be found and more readily comprehended than by looking at the original data alone" (Shi, 1993). Two-dimensional plots were made of both the localities and the taxa, showing the variance within the data sets on the two principal axes. The locality plots showed that axis 1 is generally correlated with paleo-latitude and the taxa plots showed that the same axis is correlated with an obvious transformation in foliar physiognomy from coniferophytes and cycadophytes with small leaves and thick cuticles at the low-latitude end to broad-leaved deciduous ginkgophytes at the high-latitude end. Taken together, these patterns are interpreted to indicate warm and dry conditions centered about 35°N and cool temperate conditions extending up to 80°N, with the highest-diversity warm temperate floras in the middle of the range.

In a test of consistency of the floral spectrum through time, the axis 1 scores of the adjacent intervals were correlated (Ziegler et al., 1993, fig. 1); that is, the successive ordinations were considered as duplicate samples for the purpose of comparison. That could be done because most of the genera have very extensive stratigraphic ranges. The best correlations were found in the intervals ranging from the late Triassic to the late Jurassic, so the early-middle Jurassic plot, being in the middle of the range, was selected as a sort of standard "measuring stick" for the present discussion. The individual genera were projected onto the correlation line, and a scale of 100 was superimposed. So *Zamites*, representing the low latitude end of the spectrum, was assigned the value zero, and *Phoenicopsis,* at the high-latitude end, was assigned the value 100. The "scores" for the 34 genera, derived from the plot, are given at the left side of Figure 17.1. Only the most commonly occurring genera are included in this evaluation.

The score for each taxon represents its "centroid" in the latitudinal spectrum across Eurasia, (ranging from about 30°N to 80°N), but it should be stressed that most of the forms appear in at least some of the lists from each of the three biomes. Thus *Phoenicopsis* occurs in 83% of the localities assigned to the cool temperate biome, 34% of the warm temperate localities, and 25% of the dry subtropical localities. This is due in part to the general uniformity of Mesozoic floras and in part to the time-averaging of the taxonomic lists. The gradients are subtle and can be determined only by reference to the entire assemblage. Examples of late Triassic to late Jurassic floral lists are given in Table 17.1. The average score for each list is given at the bottom of the table. But before we proceed, some caveats are discussed in the following paragraphs.

Limitations of the floral record

Late Mesozoic plant fossils are commonly preserved as impressions or coalified compressions, which, when no features (e.g., cuticle or fertile structures) are preserved to demonstrate that they are different, often leads to the creation of what are probably excessively large and artificial species (e.g., *Equisetites laterale*, *Cladophlebis denticulata, Todites williamsonii*) and genera, or form-genera (e.g., *Cladophlebis, Sphenopteris, Taeniopteris)*. That, in turn, has often given the impression of an apparent global homogeneity of Jurassic floras (e.g. Wesley, 1973).

However, the creation of a large database subjected to multivariate statistical analysis shows that this apparent homogeneity has often been exaggerated. Numerous potential problems occur, such as taphonomic bias, taxonomic inconsistency, poor stratigraphic control, uncertainty concerning the relationships of foliar organs to each other and to other plant organs, poor preservation of most material (with inferences often being made from a few specimens yielding microscopic information), and the morphological variability of different species of a given genus. However, the patterns that have emerged indicate that certain morphologies/taxa consistently co-occur. Moreover, there is a correlation between the kind of foliage preserved and its paleogeographic distribution. Combined with other geologic data, these patterns can be used to determine biomes or paleo-climatic zones.

This study, assessing co-occurrences and distributions of fossilized plant genera, is a necessary compromise. Given the subjectivity involved in assigning fossilized plant foliage at the specific level, fossil-locality assemblage lists were compiled at the generic level, taking into account the number of species per genus identified at each locality. That ensured a more standardized approach to identifications: Fossilized plant specimens are far more likely to have been assigned to the "correct" genus or form-genus than to the species; however, this entails a large degree of "slop" in the data and means that we can identify only broad phytogeographic patterns.

A major limitation of this analysis is the poor state of preservation of most of the fossilized plant assemblages. However, it is significant that foliar morphologies are similar at a given paleo-latitude, often regardless of taxonomic status. This would appear to indicate that plants developed similar strategies to maximize their efficiency in a given environment, regardless of their biological affinities. Indeed, it should be emphasized that very few fossilized plant taxa are, in fact, true biological taxa, being approximations based on morphological similarity rather than biological compatibility.

Foliar physiognomy

Figure 17.1 shows the distribution of plant genera along the floral gradient. Certain genera can be grouped together according to their morphology, which often coincides with their taxonomic classification, in this case broadly based on that of Stewart (1983). The most obvious morphological differences are seen among the conifers; small-leaved conifers with thick cuticles (coniferophyte 1) have a morphology markedly different from those with linear, abscissing leaves (coniferophyte 2). With the exception of *Elatocladus,* which is a form-genus for shoots with leaves of intermediate size, coniferophyte groups 1 and 2 are widely separated on the gradient. The ginkgophytes all group together near one end of the gradient, alongside the linear-leaved conifers. There are also morphological differences (albeit weaker) among the cycadophytes (the Cycadales and Bennettitales). Those with smaller, narrower pinnae/leaflets (cycadophyte 1) occur toward the bottom of the gradient alongside the small-leaved conifers, whereas the larger, wider forms (cycadophyte 2) occur toward the middle.

Other features of the gradient demonstrate that it is an essentially robust way of grouping and delineating genera. For instance, *Schizolepis* is a cone-scale genus that occurs among the ginkgophyte and coniferophyte-2 leaf genera. It is often found associated in fossil assemblages with leafy shoots of the coniferophyte *Pityocladus,* a genus similar morphologically to *Pityophyllum*, which lies immediately below it on the gradient. Fertile fern fronds assignable to *Todites* occur next to sterile fronds of *Cladophlebis* on the gradient; these are otherwise highly similar and usually are considered to be the fertile and sterile forms of the same plant genus. The Sphenopsida (horsetails) *Equisetites* and *Neocalamites* occur on either side of these ferns on the gradient and are highly similar, differing primarily only in the ribbing patterns on their stems.

Two genera of Gymnospermopsida (*Sagenopteris* and *Sphenopteris*) could not be subdivided or grouped with any others. Similarly, the Filicopsida (ferns) could not be subdivided on the basis of their physiognomy. Most of these genera occur in the same region of the gradient as the cycadophyte-2 group, although a few of the ferns also occur toward the higher end. *Sagenopteris* has been interpreted as colonizing environments similar to those of many ferns, typically understory sites near to water shaded by arborescent plants, whereas *Sphenopteris* is often used as a form-genus for sterile compound forms that may be ferns or pteridosperms. It is possible that ferns had a near-ubiquitous distribution, being able to colonize any environment with a water supply sheltered by arborescent forms, or else the pattern seen on the gradient may be the result of the taxonomy of ferns being relatively uncertain.

The development of small leaves and thick cuticles in the coniferophyte-1 group most probably is a response to a low availability of moisture and relatively high temperatures, and hence high evaporative stress, whereas the abscissing leaves of the ginkgophytes and coniferophyte-2 group are evidence of deciduousness, probably as a response to seasonally cool and/or dark conditions. Morphological differences within the cycadophytes are less distinct, although the forms with narrower leaflets/pinnae occur alongside the microphyllous conifers (coniferophyte 1) on the gradient, with the wider forms (cycadophyte 2) occurring towards the middle.

Some nearest living relatives

Modern cycads, represented by 11 genera, and *Ginkgo*, represented by one genus and species, are often referred to as "living fossils" because they are mere remnants of groups that dominated the vegetation in the Mesozoic. To gain insight into the habits of their forebears, we collated information on the distributions, habitats, and leaflet morphologies of the 185 species of living cycads (Jones, 1993). Of these, 172 species could be assigned a Walter biome number (Walter, 1985) according to their natural habitats. The latitudinal limits are 35°N and 35°S; so most grow in biomes 1 and 2 (tropical ever-wet and summer-wet regions, respectively). However, 31 species grow in biomes 3, 4, and 5 (subtropical desert, winter-wet/dry subtropical, and warm temperate regions), and many can tolerate conditions of seasonal aridity and even heavy frost or snow. There is a correlation between mean leaflet width and biome number; species with wide leaflets are found in biomes 1 and 2 (mean widths of 4.3 and 1.7 cm, respectively), whereas those from biomes 3 to 5 have narrow leaflets (mean widths ~ 0.8-0.9 cm), apparently related to seasonally arid and/or cooler conditions. Although all species of a particular living cycad genus tend to occur within a given biome, often there is marked variation in leaflet width between species. For example, 10 species of the genus *Dioon* all grow in Central America in biome 2, but the species with narrow leaflets grow in highly xeric areas, whereas those with wider leaflets occur in areas of less marked aridity. Additionally, one species grows in biome 1 and has the widest leaflets of any species of *Dioon.*

Such variations in modern cycads can be used to help interpret the distributions of fossil cycadophytes (including the extinct bennettites) and their relations to climate conditions in the Mesozoic. Thus, cycadophytes with narrow leaflets should tend to occur in more arid or seasonally arid regions. Indeed, there is a change in leaflet width along the floral gradient compiled for the Jurassic, with the narrowest forms at one end, co-occurring with the microphyllous

conifers, and the wider ones in the middle, warm temperate region of the spectrum. It should be noted, however, that the separation of the cycadophytes along the gradient is not as marked as that seen for the coniferophytes. Further studies are in progress on both living and fossil cycadophytes to test and refine these initial findings. This will include an assessment of morphological variation between fossilized plant species belonging to a particular genus, in an attempt to further delineate the biomes, based on the physiognomy of fossilized leaf genera.

The ginkgophytes are a group truly intermediate embryologically and morphologically between the cycadophytes and coniferophytes (Ling, 1984), and like them, diversified during the Mesozoic. The one surviving species, *Ginkgo biloba,* is now widely cultivated, but was once so close to extinction that no natural population is known for certain. The most likely indigenous population is on the 1,506-m-high Tian Mu Shan, part of an isolated mountain mass in southeast China (30°N, 119°E) (Del Tredici, Ling, and Yang, 1992). The trees occur, together with other endemic species, in an elevational range from 300 to 1200 m, where the vegetation has been interpreted as changing upslope from mixed subtropical to warm temperate, and eventually to deciduous dwarf forest above the range of the *Ginkgo.* "Under cultivation, *G. biloba* is a highly adaptable species, growing well in most parts of the world with a distinct seasonality and moderate rainfall" (Del Tredici, 1989). This includes biomes ranging from the Mediterranean to the cold temperate, and its deciduous habit is an obvious adaptation to marked summer/winter seasonality.

In view of the uncertainty surrounding the native habitat of *Ginkgo,* reference should be made to the latitudinal range of the genus as seen during its extraordinarily long stratigraphic record from the Jurassic to the Pliocene. Distributional data are available in Tralau (1968) and these have been supplemented by Neogene and Jurassic points taken from the Chinese stratigraphic literature. Tralau's data are of the highest quality, being derived from monographic treatments; our data are consistent latitudinally with his and serve simply to assure us that the genus was present in northeastern China or adjacent parts of Siberia during its entire history. All localities have been rotated to our best estimate of paleo-latitudes, and the results are shown in Figure 17.2. Clearly, *Ginkgo* has had a circumpolar distribution for most of its history, although it seems to have been progressively restricted from high latitudes in the late Tertiary, presumably as a result of lowered temperatures, as pointed out by Tralau (1968). Interestingly, the Tian Mu Shan site, at 30°N, is lower by 5° of latitude than any known earlier occurrence. One possiblity is that *Ginkgo* is not really native to this area, and the other is that it was displaced southward during one of the Pleistocene glacial intervals and was stranded on the mountain side. The survival of *Ginkgo* in China has been attributed to the relative lack of ice sheets there (Ling, 1984). The presence of endemics and its occurrence with other rare species on Tian Mu Shan would support a Pleistocene connection. In any case, the geologic record suggests that the native habit of *Ginkgo,* together with the other ginkgophytes, is in the temperate biomes. Figure 17.3 is probably an accurate depiction of variations in the latitudinal span of the cool temperate deciduous biome through time.

In summary, observations on phytogeography and foliar physignomy help to strengthen the conclusion that the observed floral gradient is related to climate zonation, particularly when the adaptations can be matched with living representatives. Moreover, the climate parameters involved can be specified to a considerable extent, and the paleogeographic distribution of the biomes shows some interesting similarities to the Recent, as well as differences. Some of the same temperate environments may be identified, such as the warm temperate and cool temperate, but they were displaced poleward in the Mesozoic, and no equivalents of the cold temperate or colder biomes have been identified. The boreal and arctic climates may have existed at inland or upland sites, but at sea level the coastal plain of the Arctic Ocean was typified by cool temperate conditions (Spicer and Parrish, 1990; Ziegler et al., 1993).

Floral data assembly

The approach in this study was to limit the sampling to 12 well-correlated basins with long records of floral accumulation; these basins are distributed from northern Europe to Siberia and China. To increase the number of taxa in the data set, collections throughout each basin or region were merged into one list within each stage-length interval, thereby coarsening the geographic resolution to hundreds of kilometers. The emphasis therefore was on temporal control, and the idea was to develop the concept of "biome stratigraphy" with exceptional case histories from a few selected areas. This can be contrasted with the geographic approach used in our earlier paper, in which the time unit was generally the epoch, averaging 10-15 m.y. (Ziegler et al., 1993). Although that earlier paper provided the standard for the floral gradient, the dictates of the present work were that the floral lists, in most cases from the same literature sources, were grouped in contrasting ways.

The incidences of the standard 34 genera of plants in the stage intervals of the 12 basins we selected are shown in Table 17.1. Correlation with the standard marine faunas in many cases was not possible, so the assignment of a flora to a particular stage was by no means certain. Moreover, the South Yakutia coal basin in Siberia was the only example in which floras from each stage in a long statigraphic sequence were recognized. The "gaps" in the other sequences do not necessarily reflect collection failure; typically, a generalized list from a single formation spanning several stages was available in the literature, and in such cases, the list was assigned to the central stage in the run. In view of these problems, the stage assignments in Table 17.1 should be regarded as entailing "plus or minus one stage."

Paleo-latitudinal paths of the Eurasian basins

In order to obtain relationships between paleo-latitudes and the floral gradients, we used paleomagnetic data to determine an appropriate reference frame. Because all continents have experienced the same magnetic-field history, they should record apparent polar-wander paths (APWPs) that differ only because of relative motions between continents. However, the paths for the major continents, as measured, are not identical, and the differences are greater than can be accounted for by uncertainties in the reconstruction parameters. Thus paleo-latitude estimates are dependent on a particular choice of reference data. Some might argue that the appropriate reference path should be derived only from Siberia, or perhaps Eurasia, where there are many published APWPs that might be used (Van der Voo, 1993). This would involve the least uncertainty, because there would be no need to transfer data from other continents. As will be clear from an examination of Figure 17.4, the APWPs for the continents included in our analysis differ, but the reasons are not clear. Rather than allowing the data from a single continent to dictate the motions of the rest, it is our preference to use a global average APWP to reduce the uncertainties within the presently available paleomagnetic inventory.

There are a few "global" paths, such as those of Ziegler, Scotese, and Barrett (1983), Besse and Courtillot (1991), and Van der Voo (1993), that could be employed, but there are several reasons for reexamining those APWPs. Clearly, the path of Ziegler et al. (1983) is out of date. The Besse and Courtillot (1991) global APWP was derived from Jurassic and Cretaceous paleomagnetic data from Africa, Madagascar, India, North America, and Eurasia that were rotated into a reconstructed coordinate frame. Means and associated statistics were computed using a 10-m.y. sliding-window average with a 21-m.y. window length. There are several reasons for not using their global APWP. First, their curve extends back only to 200 Ma, whereas we are interested in motions back to the Triassic. Enkin et al. (1992) appended a late Permian and Triassic segment to the Besse and Courtillot (1991) path using only North American and Eurasian poles and the North Atlantic reconstructions of Frei and Cox (1988). However, as noted by Nie and Rowley (1994), that incorporated substantial unacknowledged differences in North Atlantic reconstruction parameters between the Besse and Courtillot (1991) fit at 200 Ma and the Frei and Cox (1988) fit at 210 Ma. The implied motions between 210 and 200 Ma are geologically implausible, and thus an alternative approach is necessary. Second, our reconstructions of the kinematics of the breakup of Pangaea are substantially different from those used by Besse and Courtillot (1991) and thus yield different mean pole positions and associated statistics. In addition, their use of a 21-m.y. window length gave undue weight to poles for which the average age of the magnetization was assessed to fall at an even 10 m.y. That sampling bias affected 65% of their global means, although we admit that for only one mean was a 20-m.y. window-length average computed using their data and reconstruction parameters outside the 95% confidence limits of the pole that Besse and Courtillot (1991) tabulated.

Van der Voo (1993) computed both continental APWPs and a "global" APWP, but rather than employing a sliding-window averaging approach, he preferred to compute half-period interval means. He tabulated an "overall mean" based exclusively on data from North America, Europe, Africa, and South America, but only for the interval from the late middle Jurassic to the Tertiary. Because we are interested in a longer interval, it is necessary to extend the analysis back in time beyond that of Van der Voo (1993, table 6.1).

We have computed a global-average APWP based on the pole lists compiled by Van der Voo (1993) and derived from his appendix tables listing data for North America (table A1), Eurasia (table A2), Africa (table A4-I), South America (table A4-II), East Antarctica (table A5-II), and India (table A5-IV) using our own global plate-motion model. Of the poles in those lists, we have used Van der Voo's (1993) seven reliability criteria (Q) as a proxy for quality and have limited our analysis to those poles that have $Q \geq 3$, an age of magnetization adequately determined ($Q1$ checked) and assessed to be useful for APWP determination (Van der Voo, 1993). We have further restricted our selection of North American data to exclude poles derived from sites within the Basin-and-Range province of the western United States, specifically the Canelo Hills Volcanics (Kluth et al., 1982), Corral Canyon (May et al., 1986), and the Sil Nakya Formation (Kluger-Cohen, Anderson, and Schmidt, 1986), because of large uncertainties in the appropriate palinspastic restoration of these sites with respect to "stable" North America. This is more restrictive than the data base employed by Van der Voo (1993), specifically by requiring the age of magnetizaton to be well determined, and by excluding poles from the Basin and Range region.

The approach that we adopted to compute our global APWP was to determine 20-m.y. sliding-window (or interval) means for each of the continents listed earlier at 10-m.y. time steps using standard Fisher statistics. Table 17.2 lists the poles that were used, together with their rotated coordinates in a European reference frame, for each of the appropriate interval windows. All poles have been rotated into a common reference frame (Europe) using the reconstruction parameters listed in Table 17.3. Note that the approach is to rotate each pole using rotation parameters appropriate to the time of the interval midpoint. All poles on the same block preserve their present unrotated relative positions, and hence the choice of reference frame does not influence the statistics associated with a given collection of poles. This allows the interval means to be directly calculated within the appropriate frame of reference. This contrasts with the approach used by Besse and Courtillot (1991), who rotated each pole into a common reference frame using rotation parameters appropriate to the mean age of magnetization for each pole. That resulted in changes in the relative positions of poles from the same block, and consequently changes in the global mean statistics in each reference frame. A similar problem would result if one

simply used the rotated paleo-poles of Van der Voo (1993), as listed, for example, in his table A4 for western Gondwana.

Table 17.4 lists poles along three alternative global APWPs, as well as each of the continental means in a Eurasian reference frame based on the poles in Table 17.2. The interval means for each continent are determined using standard paleomagnetic statistical procedures. The three global APWP poles are determined using different approaches to clustering the data, in turn reflecting different assumptions concerning the relative weighting of the data. The computation of the global means in these different ways reflects the fact that there have been variable levels of investigation of these continents and that the estimate of the uncertainty of the mean (A95) is inversely proportional to *N* (the number of poles). The "global study means" in Table 17.4 are the means and associated statistics of all studies listed in Table 17.2 that fall within a given 20-m.y. window. The "unweighted global means" in Table 17.4 are computed by determining the interval means for each continent and then computing grand interval means, with each continent having the same weight. The "weighted global means" in Table 17.4 are computed by determining the interval means for each continent and then computing weighted grand interval means. We employ a weighting scheme that depends primarily on the number of studies that contributed to each of the continental interval means, rather than giving the same weight to each continent irrespective of how well determined its mean might be. Thus continents with interval means determined from fewer than 5 studies are counted once, 5 to 10 are counted twice, and 10 or more are counted three times. This allows those continents with abundant data to have proportionately greater influence on the global interval mean position. Although there are generally relatively small differences in the global APWP pole positions among these various approaches, the primary difference is in the estimated uncertainty (A95) of the various poles, reflecting differences in *N*. The cutoffs mentioned above are arbitrary, but are chosen so as to maintain *N* sufficiently small that A95 will still be large. Table 17.5 summarizes this aspect of our results. Our preferred global APWP is the weighted global continental mean path shown in Figure 17.5. Our preference is based on the comparisons of the relatively large (~ 7°) average A95 with the average angular distance (~ 7.9°) of the continental interval means from the weighted global continental mean, and to the mean A95 of the individual studies of about 7° that contribute to continental interval means.

The stage-by-stage paleo-latitudinal paths of the eight Eurasian basins are shown in Figure 17.6, based on our preferred global APWP. Eurasia is represented by France and Britain, and the former U.S.S.R. by South Yakutia, Transbaikalia, Kuzbass (Kuznetsk Basin), the eastern Urals, Fergana, and Karatau. The latter two are very close together and constitute duplicate samples; the Fergana list is a composite of several basins ranging over several hundred kilometers, and the Karatau list is much more geographically restricted. All of the foregoing northern Eurasian sites have been treated as belonging to a single plate in the Mesozoic and Cenozoic.

Paleo-latitudinal calibration of the floral gradient

The floral-gradient scores for northern Eurasia (Table 17.1, bottom row) have been plotted against the paleo-latitude appropriate for each sample (from Figure 17.6), as shown in Figure 17.7. A reasonable correlation exists, particularly in the middle of the range. The European points at the low end are more scattered, and it is possible that future studies will show a "hook" in the curve in the tropical region such that samples on the equatorial margin of the desert zone will have gradient scores similar to those for the warm temperate samples. This would imply that the floras at low latitudes were dominated by precipitation, and those at high latitudes by temperature. This would be simply a reflection of the fact that precipitation does not vary monotonically with latitude, whereas temperature does.

The scores for the Siberian points at the high end of the spectrum are less variable than might be expected from their paleo-latitudinal range. It may be that a convex-upward curve should be fitted to this portion of the distribution and that the high-latitude end is less useful as a paleo-latitudinal measure. Here the length of the growing season, as influenced by temperature or the duration of the polar night, probably is the controlling factor. There is no guarantee that this effect will be directly proportional to latitude.

There is possibly some temporal variation in the floral gradient related to the degree of continentality that seems to have decreased through the interval of interest. Various authorities agree that sea level was low in the late Triassic and early Jurassic through the Pliensbachian stage, that it was moderate through the Bathonian stage of the middle Jurassic, and that it was high for the rest of the period (Hallam, 1992, fig. 4.5). One might predict that cooler floras would occur at lower latitudes during times of high continentality, and such a correlation is evident at least for the times of lowest sea-level (Figure 17.7). We also categorized the floras on the basis of depositional setting -- coastal plain or continental interior -- but no difference was apparent in the slopes of the curves. Because maritime climates typically are milder than interior climates, that was an attempt to determine if we could observe such a trend in our data. Because this study is preliminary and is to be followed by a much more extensive survey already underway, the conclusions and speculations in this chapter are subject to revision. At this time we fall back to the correlation line in Figure 17.6 and accept this as our standard for the latitudinal calibration of the floral gradient.

Taken together, the 12 basins represent a latitudinal spectrum of about 65° or 7,000 km, ranging from the tropics to near the pole (Figure 17.3). The latitudinal span is wider in the late Triassic and early Jurassic because Eurasia was tilted to the northeast. By the late Jurassic it had rotated clockwise to approach its present east-west orientation, and the latitudinal range of the basins had been reduced to about 35°.

Tectonic relationships of the Chinese microcontinents

Recently a paper appeared that was entitled "Paleomagnetic Constraints on the Geodynamic History of the Major Blocks of China from the Permian to the Present" (Enkin et al., 1992). Those authors reviewed the available poles and constructed APWPs for the major blocks. They presented maps to show that the Chinese poles do not superimpose on the northern Eurasian poles for intervals prior to the lower Cretaceous, and they reconstructed the paleogeography with the Chinese elements in contact with Eurasia throughout, but with large intermediate ocean basins that closed rotationally through the Triassic and Jurassic. Nie and Rowley (1994) commented, "that it is premature to present overly detailed paleogeographic reconstructions or postulate major sutures, despite their incompatibility with existing geological data, to accommodate motions just to fit the still quite limited paleomagnetic data." They pointed out that 2,000 km of convergence of North China and Siberia is implied by the paleomagnetic data in the late Jurassic, when full suturing was complete (Parfenov and Natal'in, 1985). The Enkin et al. (1992) reconstructions would place North and South China in the subtropics through the Jurassic, and that is at variance with the temperate nature of the floras (Ziegler et al., 1993); so the magnitude of the discrepancy is considerable and is testable using the floral-gradient-derived paleo-latitudes.

In our floral dataset, China is represented by Tarim (a small microcontinent in central Asia), by Sichuan and Fujian provinces on opposite sides of the South China microcontinent, and by the Ordos basin of the North China microcontinent. Because the Chinese microcontinents are surrounded by deformed oceanic sediments, their positions with respect to the rest of the world are difficult to determine precisely.

The approach that was followed in generating the reconstructions presented in Figure 17.8 was to evaluate regional geologic information pertaining to the nature, timing, and magnitude of deformation represented by the larger-scale structures within Asia, as part of global compilations of the Paleogeographic Atlas Project; see Nie and Rowley (1994) and Ziegler et al. (1985) for a summary of our approach. We mapped these features on a scale of $1{:}10^6$ and then attempted a first-order palinspastic restoration of the kinematics to arrive at a model for the deformation history and its implications for the paleogeographic reconstructions. This process does not necessarily take the existing paleomagnetic data into direct consideration at all stages, as is clear from the divergence of interpretations based largely on the paleomagnetic data (e.g., Enkin et al., 1992) versus those based on regional kinematics (Rowley, 1992). It is beyond the scope of this chapter to summarize all of the data pertaining to each of the regional structures; however, it seems important to provide some overview of the bounds on viable reconstructions that have been imposed by the regional geology. We start in the north and work southward.

Mongol-Okhotsk suture

For the purposes of this chapter, perhaps the most important boundary is what Kosygin and Parfenov (1981) and Natal'in and Parfenov (1985) referred to as the Dzhagdi suture, but which others have variously named the Shilka suture (Klimetz, 1983) or the Mongol-Okhotsk belt (Zonenshain et al., 1990), the name we shall adopt here. This suture is critical because it is the only post-Paleozoic suture that extends westward into Central Asia north of the North China block and the only post-Triassic suture north of the Banggong-Nujiang suture in central Tibet (Chang and Cheng, 1973; Chang, Pan, and Sun, 1989). This boundary represents the most likely place across which large (>10°) paleo-latitudinal disparitites would occur. The Mongol-Okhotsk suture has figured prominently in a number of attempts to reconstruct the paleogeographic evolution of this part of Asia (Rowley et al., 1985; Nie et al., 1989; Rowley, 1992; Sengör, Natal'in, and Burtman, 1993). The Mongol-Okhotsk suture is a narrow zone characterized by oceanic sediments of Paleozoic to mid-Mesozoic age surrounded on three (N, W, and S) sides by pre-Altaid continental crust that underlies the Tuva-Mongol block *sensu stricto* of Sengör et al. (1993). The western extent of the Mongol-Okhotsk suture is limited by this basement at about 47°N, 98°E, where the former oceanic domain is represented by the Khangai zone of Zonenshain et al. (1990). Many of the units entrained within the Mongol-Okhotsk suture are older Paleozoic and even late Precambrian in age, but thick marine clastics, olistostromes, mafic complexes, and melanges of Triassic and Jurassic age are extensively preserved as well (Marinov, Zonenshain, and Blagonravov, 1973; Parfenov and Natal'in, 1985; Zonenshain et al., 1990).

The marine Mesozoic units continue the depositional patterns of the middle and late Paleozoic, except that they are restricted to more easterly regions of the Mongol-Okhotsk belt. These Mesozoic units were variably deformed by the Cretaceous (Zonenshain et al., 1990). Nie, Rowley, and Ziegler (1990), following Rowley et al. (1985), argued that the termination of the Mongol-Okhotsk basin in the west necessitates that it close in a scissor-like fashion, such that subduction and associated deformation terminate diachronously along the belt, from Permo-Carboniferous in the west to Jurassic in the east. Late Permian and early Cretaceous paleomagnetic data from the eastern Altaid region (Pruner, 1987) and the North China block (Zhao and Coe, 1987; Enkin et al., 1992) are broadly compatible with this interpretation. Furthermore, late Jurassic surficial deposits are widely distributed throughout the area of Mongolia and are entirely terrestrial (Marinov et al., 1973), and hence the "south-verging suture(?)" surmised by Enkin et al. (1992) as extending from "the Verkhoyansk range in the east to the Sayan range in the west" is contradicted by the geologic record.

The Mongol-Okhotsk belt extends some 3,000 km into Asia from the coast. Thus, the maximum latitudinal difference between points situated on North China or the

northeast China fold belt is about 30° from what would be predicted by Eurasian or Siberian paleomagnetic data. This assumes that there has been little net contraction or elongation of the Altaid region north of the North China block in post-Permian times. The deformation history of this region is complex, including both folding and extension. The extension within this domain is perhaps more obvious, as shown by the development of a large number of basins, including the Sanjiang, Songliao, Hailar, and Erlian basins of Jurassic to early Cretaceous age (Tang et al., 1988; Zhang et al., 1993; Wang, Yang, and Gao, 1993). These basins are controlled by approximately NE-SW faults, indicating net elongation of the region south of the Mongol-Okhotsk suture. This would imply a shorter original arc length and hence that the latitudinal difference between North China and Eurasia was less than 30°. As we do not know the balance between early shortening and later extension, the present 30° difference seems a reasonable limit. It is also important to note that the eastern Altaid folded region and the North China block had already collided with each other by late Permian time (Ishii et al., 1991). This is demonstrated by the widspread distribution of non-marine Permian sediments across the North China fold belt, resting above angular unconformities, with older Paleozoic units below (Nei Mongol Stratigraphic Group, 1978; Heilongjiang Stratigraphic Group, 1979). The progressive, diachronous eastward closure of the Mongol-Okhotsk suture and the contiguity of North China and the Altaid region situated south of the suture places severe limitations on acceptable reconstruction of North China relative to Eurasia following the middle Permian. The presence of Triassic and Jurassic arc-related magmatism north of the suture implies continuous closure of the Mongol-Okhotsk ocean through that interval, supporting observations of the progressive restriction of marine sediments to more easterly regions of the suture. Thus the angular separation across the Mongol-Okhotsk ocean must have decreased with time, and it would have been fully closed along all but the last few hundred kilometers by the end of the Jurassic (Kosygin and Parfenov, 1981; Parfenov and Natal'in, 1985). In our model we treat the rotational closure as occurring at a constant rate. The pole of rotation for this closure cannot be fixed to its western termination, as might initially be assumed. This is because such a pole would imply equal magnitudes of extension to the south and west, as well as contraction to the north and east. Thus the 90° or more of rotation of North China relative to Siberia in Triassic and Jurassic times is not balanced by an equivalent magnitude of extension about such a pole. Hence, the system must include more than two plates, or the pole must lie outside the crust that comprises the Altaid region south of the Mongol-Okhotsk suture, not to mention all of the crust farther to the south to the next plate boundary, which for Triassic times would be the Qinling-Kunlun suture, but for post-Triassic times would be the Banggong-Nujiang suture. For the reconstructions presented in Figure 17.8, we stress the latter option in our model of the counterclockwise rotation to close the Mongol-Okhotsk suture. As all of west-central China south to the Banggong-Nujiang suture within Tibet is characterized by Triassic through mid-Jurassic contractional deformation, not extension, the pole must be situated to the southwest sufficiently far that extensional deformation is not implied for this region. Note that we have phrased this discussion in terms of plates, but in view of the regionally distributed deformation, it is clear that this region did not behave rigidly. We have simplified the system to this level in order to describe the relative motions in such a way that computer mapping techniques can approximate the deformation field.

Qinling-Dabie Shan-Sulu suture

South China collided with North China along the Qinling-Dabie-Sulu suture during the Triassic. The closure occurred first in the east and then proceeded diachronously westward. This is demonstrated by the presence of coeval middle Triassic marine carbonates in the Qinling immediately south of the suture in the west, and by the 240-220Ma Sm-Nd ages on the continental-crust-derived ultra-high-pressure metamorphic rocks within the Dabie Shan and Sulu regions in the east (Li et al., 1989a,b, 1993; Li and Liu, 1990; Okay, Sengör, and Satir, 1993). The middle Triassic carbonates in the Qinling demonstrate that collision-related loading and syn-orogenic sedimentation had not yet affected that region and thus that the collision there must post-date the middle Triassic, whereas the age data on collision-related metamorphism indicate that collision was well under way at more easterly longitudes. This diachroneity is further supported by the angular discordance between North China and South China late Permian and early Triassic paleomagnetic data (Zhao and Coe, 1987; Nie, 1991; Enkin et al., 1992). Contractional deformation continued after collision within the Qinling-Dabie Shan area through the Upper Triassic and into the lowermost Jurassic. However, the widespread angular unconformity separating upper Lower to Middle Jurassic units from underlying strata along the southern flanks of the Qinling-Dabie Shan, as well as within and to the north, documents this early phase of deformation within the Qinling-Dabie Shan region. These unconformities were subsequently folded, with the highest stratigraphic units involved in the folding being late Jurassic and early Cretaceous (Jiangxi Bureau of Geology and Mineral Resources 1984; Anhui Bureau of Geology and Mineral Resources, 1987; Henan Bureau of Geology and Mineral Resources, 1989; Shaanxi Province Bureau of Geology and Mineral Resources, 1989; Hubei Bureau of Geology and Mineral Resources, 1990; Sichuan Bureau of Geology and Mineral Resources, 1991). Unfortunately, reliable estimates of the total shortening within the Qinling are not available. The southern Qinling and central Qinling are about 250 km wide, perpendicular to the regional NW-SE strike. Assuming 50% shortening, a plausible estimate of the pre-collisional width of the southern Qinling basin would be about 500 km. A similar magnitude of shortening is required within the Dabie Shan in order to yield the present horizontal gradient of metamorphic pressures and their syn-kinematic exhumation (Rowley, 1995). Given the existing data, it is not

clear that there has been a significant (>10°) component of post-late Triassic rotation absorbed within the Qinling-Dabie Shan orogen. In our model, North China and South China are held fixed with respect to each other in post-Triassic time. This certainly is not correct in detail, but the magnitude of the N-S component of motion is probably less than 5°, and motions along the large, presently east-west strike-slip faults would not have resulted in significant latitudinal motions.

Tarim

For the purposes of this chapter, focussing on the Triassic and Jurassic position of Tarim relative to Eurasia, we have assumed that Tarim and Eurasia collided late in the early Permian and that it subsequently underwent counterclockwise convergence in mid-Permian to Jurassic time. There is clear evidence in the stratigraphy of the surrounding basins for the development of extensive foreland basins associated with thrust loading and shortening within the Tien Shan (Hendrix et al., 1992). Late Permian paleomagnetic data from opposite sides of the Tien Shan (Li et al., 1988, 1991; McFadden et al., 1988; Nie et al., 1992) suggest that Tarim and at least the Bogda Shan have not experienced significant post-late Permian convergence, and that is compatible with the geology of this area.

Comparison of the Chinese and Eurasian paleomagnetic results

Significant Mesozoic and Cenozoic deformation has affected virtually all of China. There are only very limited "stable" components, such as the center of the Sichuan, Ordos, and Tarim basins, that have not experienced significant post-Paleozoic deformation. Thus, virtually all paleomagnetic sites in China are from deformed areas that may have undergone significant rotations relative to each other. So, unlike North America or Europe, where it is possible to establish a reasonably stable framework for comparison of findings from adjacent deformed domains, as, for example, was done by Bryan and Gordon (1988) with the paleomagnetic data from the Colorado Plateau, it may not be possible to determine the effects of significant rotational components of this deformation on the Chinese paleomagnetic data. Enkin et al. (1992) noted this and pointed out that poles of a given age tend to be distributed along small circles at relatively constant inclination, and not to be clustered about their means. Because there is no stable framework, the approach that has been implicitly adopted has been to assume that the poles have been distributed equally away from the "real" mean, and hence that the mean of the distribution has been a reasonable representation of the blocks' orientations (mean declinations) relative to paleo-latitude. This need not be the case, particularly for the late Permian of South China, because many of the findings are from virtually a single site at Emei Shan in eastern Sichuan Province. This is true, perhaps to a lesser extent, for other times and blocks, reflecting the still-limited inventory of paleomagnetic data.

Figure 17.8 also plots the paleo-latitudinal positions of South China and North China according to the mean poles determined from their paleomagnetic data, tabulated by Enkin et al. (1992, table 2). The discrepancy is obvious between these positions and the predictions based on our simplified kinematic modeling and reconstruction of the global mean APWP. The plots show the disparities for certain intervals very clearly, whereas for others the data fit reasonably well. It should be noted that for the late Permian, the reconstructions explicitly acknowledge the paleomagnetic data for South China and Tarim, and hence the fit is by design. There are numerous potential sources of misfit of the geologic and paleomagnetic data. We prefer the approach of emphasizing the geologic information over the existing paleomagnetic data at this time, as the post-early Triassic data are still very limited, and (as is clear from these figures) the existing data, if followed rigidly, do not place North China and South China in their correct N-S order in post-middle Triassic times. Thus the reconstructions portrayed by Enkin et al. (1992) are not based on the means, but rather incorporate some significant prejudices, presumably predicated on the geologic evolution of this region. Thus, in our view, the geologic data, particularly the absence of plate-scale boundaries internal to eastern Asia, preclude accommodation of the large latitudinal displacements implied by the existing paleomagnetic data. It is worth noting, as well, that although the data incorporated in the global APWP determination cluster quite well, for most intervals there remains significant dispersion of continental means. Hence the rigorous comparison of the means from different blocks overstates the fidelity with which the APWPs of continents with well-determined relative positions compare.

The stage-by-stage paleo-latitudinal paths of the four Chinese basins are shown in Figure 17.3, based on our preferred global APWP and our reconstructions of the deformation history of eastern Asia. The South China comparison of the floral-gradient-derived latitude with the tectonic- and paleomagnetic- based (Enkin et al., 1992) reconstructions shows good support for the tectonically conservative approach (Figure 17.9a,b). The same is true for North China (Figure 17.9c), whereas the paleo-latitude of Tarim may have been underestimated 4° or 5° by the tectonic approach (Figure 17.9d). In most cases, the error bars on the paleomagnetic data are so large that they overlap the floral determinations, but still they are consistently low and range from 1,000 km to 3,000 km south of the position suggested by the floras and the tectonic constraints.

Much effort will be required to firm up the floral and paleomagnetic data before the differences are resolved. We are convinced, however, that the tectonically conservative approach has its merits and that the climatically sensitive sediments and floras can be relied on to track the latitudinal progression of the Chinese microcontinental elements. North China and South China were both near the equator in the Permian, as indicated by the equatorial rainforest floras, and North China did not approach the Northern Hemisphere desert zone until the latest Permian (Ziegler, 1990). Evaporites and "arid-terrestrial" sediments are present in the

Lower and Middle Triassic (Wang, l985), indicating the passage of both North China and South China through the subtropics. Note that this is the latitudinal band in which Enkin et al. (1992) would place these blocks as late as the Jurassic. However, coals are widespread throughout China in Upper Triassic and Lower Jurassic rocks, giving us confidence that these areas had crossed the desert belt and were in the temperate rainy zone by that interval, as suggested by the floras.

There is general agreement that the Permian paleomagnetic data for South China and North China are numerous, reliable, and confirmable by the equatorial floras and sediments (Nie et al., 1990; Enkin et al., 1992.). The Lower Triassic poles are also numerous and most have been determined from the basal formation of the epoch; so it is not surprising that they are similar to the Upper Permian poles. The Middle and Upper Triassic poles, on the other hand, are limited to a few representing a very long time interval, and it is here that future paleomagnetic studies could be directed to advantage. The Jurassic poles are fairly numerous, but very similar to the Cretaceous poles, and here we suspect that the magnetic directions of these continental strata were reset in late Mesozoic times. In our view, they underestimate the paleolatitude by about 20° in the Jurassic.

Conclusions

Despite the relatively subtle temperature gradients apparent for the early Mesozoic, floral variations did occur and can be employed to measure spatial and temporal climate changes. Individual genera can be seen in just about any list, but the climate signal is lodged in the sum total of the floral elements. Moreover, consistency of the floras through long intervals of geologic time is evident with or without the multivariate analysis. The statistical approaches allow for construction of an objective scale to compare the floras. However, anyone can place a taxonomic list on the gradient by simply averaging the scores for all of the 34 genera occurring in the list. This study is a preliminary one, but it demonstrates that it is possible to sort out the multiple effects of climate change, continental motions, and floral evolution.

Studies with larger data sets are planned to examine the latitudinal adjustments of the floral gradient through time. There is a hint in the present work that the times of highest continentality coincided with the steepest gradients. Also, the changes in the latitudinal range of the genus *Ginkgo* over the past 200 m.y. are consistent with expectations from other paleoclimate studies (Markwick, 1994), suggesting that the changes were in the climate, not in the preferences of *Ginkgo*. Care must be taken to differentiate between real global change and the effects produced when a continent passed beneath climate zones. The climate of Asia became warmer and drier through the middle and late Jurassic, whereas the reverse was true of North America. Thus, the sandy deserts of the Navajo and Entrada Formations of the early and middle Jurassic (Parrish and Peterson, 1988) gave way to the seasonally wet climates of the Morrison Formation of the late Jurassic (Dodson et al., 1974), and finally to the temperate coal swamps of the Cretaceous (Horrell, 1991). It should be noted that changes in the Mesozoic floras and faunas, using mainly North American examples, have been interpreted as the results of evolution (Wing and Tiffney, 1987) rather than of climate. The clockwise motion, about an axis in Europe, resulted in a poleward motion of North America, and the reverse in eastern Asia. The latitudinal transitions in the floras stayed about the same, so we would maintain that no net global change occurred in the areas occupied by the individual biomes. Evolutionary studies should therefore be limited initially to within-biome comparisons.

The paleo-latitudinal paths of the South and North China microcontinents can be reliably reconstructed from the changes in climate reflected in the floras and sediments. Nie (1991) was able to show this for the Paleozoic, and our Mesozoic paths are simply continuations of his earlier trajectories, which ended with the collisions of the blocks that became parts of Eurasia at the end of the Jurassic. We are uncertain why the paleomagnetic study of Enkin et al. (1992) underestimated the paleo-latitudes of these blocks by as much as 20°. The poles may have been reset, the age assignments may have been otherwise incorrect, or the data simply may have been too few for reliable averages.

Acknowledgments

Thanks are due to Professor R.A. Spicer of the Open University for early help in developing the floral-gradient approach used in this study. Guang Yang of the Jiangsu Institute of Botany, Nanjing, kindly provided a number of his translations of Chinese articles on *Ginkgo*. The funding that made this work possible was provided by the following companies: Agip, Amoco, BHP-Utah, Exxon, Mobil, Petrobras, Shell, Total, and Union Texas. D. Rowley acknowledges R. Van der Voo for providing an ASCII version of his appendix tables and NSF grant EAR-9206523 for support of Chinese paleomagnetic investigations.

References

Anhui Bureau of Geology and Mineral Resources, 1987, Regional Geology of Anhui Province (in Chinese with English summary): Beijing, Geological Publishing House.

Besse, J. and Courtillot, V., 1991, Revised and synthetic apparent polar wander paths of the African, Eurasian, North American and Indian plates, and true polar wander paths since 200 Ma: Journal of Geophysical Research, v. 96, p. 4029-4050.

Bryan, P., and Gordon, R. G., 1988, Rotation of the Colorado Plateau: an updated analysis of paleomagnetic data: Geological Society of America Abstracts with Programs, v. 20, p. A63.

Bureau of Geology and Mineral Resources of Jilin Province, 1988, Regional geology of Jilin Province (in Chinese with English summary), *in* People's Republic of China

Ministry of Geology and Mineral Resources Geological Memoirs, Series 1, No. 10, 698 p.

Chang, C. F., and Cheng, H. L., 1973, Some tectonic features of the Mt. Jolmo Lungma area, southern Tibet: Sciencia Sinica, v.14, p. 247-265.

Chang, C. F., Pan, Y. S., and Sun, Y. Y., 1989, The tectonic evolution of the Qinghai-Tibet Plateau: a review, *in* Sengör, A. M. C., ed., Tectonic Evolution of the Tethyan Region: Norwell, Massachussetts, Kluwer, p. 415-476.

Del Tredici, P., 1989, Ginkgos and multituberculates: Evolutionary interactions in the Tertiary, *in* BioSystems: Ireland, Elsevier Scientific Publishers Ireland Ltd., p. 327-339.

Del Tredici, P., Ling, H. and Yang, G., 1992, The ginkgos of Tian Mu Shan: Conservation Biology, v. 6, p. 202-209.

Dobruskina, I. A., 1982, Triassic flora of Eurasia (in Russian): Trudy Akademii Nauk SSSR, Seria geologicheskaya, v. 365, p. 1-195.

Dodson, P., Baker, R.T., Behrensmeyer, A.K. and McIntosh, J.S., 1974, Paleoecology of the dinosaur-bearing Morrison Formation: National Geographic Society Research Reports, v. 15, p. 145-156.

Enkin, R.J., Yang, Z.Y., Chen, Y. and Courtillot, V., 1992, Paleomagnetic constraints on thegeodynamic history of the major blocks of China frm the Permian to the Presesnt: Journal of Geophysical Research, v. 97, p. 13,953-13,989.

Frei, L., and Cox, A., 1988, Relative displacement between Eurasia and North America prior to the formation of oceanic crust in the North Atlantic: Tectonophysics, v.142, p. 111-136.

Gauch, Jr., H.G., 1982, Multivariate Analysis in Community Ecology, *in* Beck, E.,H.J.B. Birks, H.J.B. and Connor, E.F., eds, Cambridge Studies in Ecology: New York, Cambridge University Press, 298 p.

Hallam, A., 1992, Phanerozoic sea-level changes, *in* Bottjer, D. and Baumbach, R.K., eds. The Perspectives in Paleobiology and Earth History Series: New York, Columbia University Press, 266 p.

Hallam, A., 1993, Jurassic climates as inferred from the sedimentary and fossil record, Philosophical Transactions of the Royal Society of London B, v. 341, p. 287-295.

Hebei Stratigraphic Group, 1979, Regional Stratigraphic Data of Northern China(Hebei) (in Chinese), v. 1: Geology Press, 312 p.

Heilongjiang Stratigraphic Group, 1979, Regional Stratigraphic Data of Northeastern China (Heilongjiang): Beijing, Geological Publishing House, 299 p.

Henan Bureau of Geology and Mineral Resources, 1989, Regional Geology of Henan Province (in Chinese with English summary): Beijing, Geological Publishing House, 772 p.

Hendrix, M. C., Graham, S. A., Carroll, A. R., Sobel, E. R., McKnight, B. J., and Schulein, B.J., 1992, Sedimentary record and climatic implications of recurrent deformation in the Tian Shan: Evidence from Mesozoic strata of the Tarim, south Junggar, and Turpan basins, northwest China: Geological Society of America Bulletin, v.104, p. 53-79.

Horrell, M.A., 1991, Phytogeography and paleoclimatic interpretation of theMaestrichtian: Palaeogeography, Palaeoclimatology, Palaeoecology, v. 86, p. 87-138.

Hubei Bureau of Geology and Mineral Resources, 1990, Regional Geology of Hubei Province (in Chinese with English summary): Beijing, Geological Publishing House, 705 p.

Ishii, K.-I., Wueya, L., Koichiro, I., and Huang, B.H., eds., 1991, Pre-Jurassic Geology of Inner Mongolia, China: Report of China-Japan Cooperative Research Group, 1987-1989: Osaka, China-Japan Cooperative Research Group, 236 p.

Jiangxi Bureau of Geology and Mineral Resources, 1984, Regional Geology of Jiangxi Province (in Chinese with English summary): Beijing, Geological Publishing House, 921 p.

Jilin Stratigraphic Group, 1978, Regional Stratigraphic Data of Northeastern China(Jilin) (in Chinese): Geology Press, 214 p.

Jones, D.L., 1993, Cycads of the World: Ancient Plants in Today's Landscape: Washington, D.C., Smithsonian Institution Press, 312 p.

Klimetz, M. P., 1983, Speculations on the Mesozoic plate tectonic evolution of eastern China: Tectonics, v.2, p. 139-166.

Kluger-Cohen, K., Anderson, T. H., and Schmidt, V. A., 1986, A paleomagnetic test of the proposed Mojave-Sonora megashear in northwestern Mexico: Tectonophysics, v.131, p. 23-51.

Kluth, C. F., Butler, R., Harding, L. E., Shafiquallah, M., and Damon, P. E., 1982, Paleomagnetism of Late Jurassic rocks in the northern Canello Hills, southeastern Arizona: Journal of Geophysical Research, v.87, p. 7079-7086.

Kosygin, Y. A., and Parfenov, L. M., 1981, Tectonics of the Soviet Far East, *in* Nairn, A. E. M., Churkin, M. and Stehli, F.G., eds., The Ocean Basins and Margins: New York, Plenum, p. 377-412.

Krassilov, V.A., 1981, Changes of Mesozoic vegetation and the extinction of dinosaurs: Palaeogeography, Palaeoclimatology, Palaeoecology, v. 34, p. 207-224.

Li, S., Ge, N., Liu, D., Zhang, Z., Yie, X., Zhen, S., and Peng, C., 1989a, Sm-Nd age of c-group eclogites in northern Dabie Mountains and its tectonic significance: Bulletin of Science, v. 7, p. 522-525.

Li, S., Hart, S. R., Chen, S., Guo, A., Liu, D., and Zhang, Z., 1989b, Sm-Nd age for the collision between Sino-Korean and Yangtze cratons: Academia Sinica, v. 2B, p. 312-319.

Li, S., and Liu, D., 1990, Isotopic chronological evidence for Indosinian orogeny in the Dabie Mountains: Geotectonica et Metallogenica, v.14, p. 159-163.

Li, S. G., Xiao, Y. L., Liou, D. L., Chen, Y. Z., Ge, N. J., Zhang, Z. Q., Sun, S. S., Cong, B. L., Zhang, R. Y., Hart, S. R., and Wang, S. S., 1993, Collision of the North China and Yangtse blocks and formation of coesite-bearing eclogites: timing and processes: Chemical Geology, v. 109, p. 89-111.

Li, Y., McWilliams, M. O., Cox, A., Sharps, R., Li, Y. A., Gao, Z., Zhang, Z., and Zhai, Y., 1988, Late Permian paleomagnetic pole from dikes of the Tarim craton: Geology, v. 16, p. 275-278.

Li, Y., Sharps, R., McWilliams, M. O., Li, Y., Li, Q., and Zhang, W., 1991, Late Paleozoic paleomagnetic results from dikes of the Junggar block, northwest China: Earth and Planetary Science Letters, v. 94, p. 123-130.

Liaoning Stratigraphic Group, 1978, Regional Stratigraphic Data of Northeastern China (Liaoning) (in Chinese): Geology Press, 296 p.

Ling, H., 1965, Origin and distribution of Ginkgo biloba: Bulletin of Biology, v. 3, p. 32-33.

Ling, H., 1984, The living fossil--Ginkgo biloba L.: Journal of Biology Teaching, v. 3, p. 17-18.

Marinov, N. A., Zonenshain, L. P., and Blagonravov, 1973, Geology of the People's Republic of Mongolia: Stratigraphy, Moscow, 582 p.

Markwick, P.J., 1994, "Equability", continentality, and Tertiary "climate": The crocodilian perspective: Geology, v. 22, p. 613-616.

May, S. R., Butler, R., Shafiquallah, M., and Damon, P. E., 1986, North American Jurassic apparent polar wander: implications for the North American 170 Ma reference pole: Journal of Geophysical Research, v.91, p. 11545-11555.

McFadden, P. L., Ma, X., McElhinny, M. W., and Zhang, Z., 1988, Permotriassic magnetostratigraphy in China: northern Tarim: Earth and Planetary Science Letters, v. 87, p. 152-160.

Meyen, S.V., 1987, Fundamentals of Palaeobotany: London, Chapman and Hall, 432 p.

Nei Mongol Autonomous Region Bureau of Geology and Mineral Resources, ed., 1991, Regional Geology of Nie Mongol (Inner Mongolia) Autonomous Region (in Chinese with English summary): People'sRepublic of China Ministry of Geology and Mineral Resources Geological Memoirs Series 1, Number 25, 724 p.

Nei Mongol Stratigraphic Group, 1978, Regional Stratigraphic Data of Northern China (Nei Mongol): Beijing, Geological Publishing House, 338 p.

Nie, S.Y., 1990, Constraints on the Paleozoic plate reconstructions of China: Ph D. dissertation, v. 1 and 2, 321 p.

Nie, S.Y., 1991, Paleoclimatic and paleomagnetic constraints on the Paleozoic reconstructions of south China, north China and Tarim: Tectonophysics, v. 196, p. 279-308.

Nie, S.Y. and Rowley, D.B., 1994, Tectonic evolution of eastern Asia--A comment on "Paleomagnetic constraints on the geodynamic history of the major blocks of China from the Permian to the Present" by Enkin et al.: Journal of Geophysical Research, v. 99, p. 18,038-42.

Nie, S.Y., Rowley, D.B. and Ziegler, A.M., 1990, Constraints on the locations of Asian microcontinents in Palaeo-Tethys during the Late Palaeozoic, *in* McKerrow,W.S. and Scotese, C.R., eds., Palaeozoic Palaeogeography and Biogeography: Geological Society Memoir No. 12, p. 397-409.

Nie, S. Y., Van der Voo, R., Rowley, D.B., and Li, M., 1992, Paleomagnetism of late Paleozoic rocks of the Tianshan, northwest China: Tectonics, v. 11, p. 568-579.

Ningxia Stratigraphic Group, 1980, Regional Stratigraphic Data of Northwestern China(Ningxia) (in Chinese): Geology Press, 188 p.

Okay, A. I., Sengör, A. M. C., and Satir, M., 1993, Tectonics of an ultra-high-pressure metamorphic terrane: The Dabie Shan/Tongbai Shan orogen, China: Tectonics, v. 12, p.1320-1334.

Parfenov, L. M., and Natal'in, B. A., 1985, Mesozoic accretion and collision tectonics of northeastern Asia, *in* Howell, D. G., ed., Tectonostratigraphic Terranes of the Circum-Pacific Recgion: Houston, Texas, Circum-Pacific Council of Energy and Mineral Resources, p. 363-373.

Parrish, J.T. and Peterson, F., 1988, Wind directions predicted from global circulation models and wind directions determined from eolian sandstones of the western United States--A comparison: Sedimentary Geology, v. 56, p. 261-282.

Pruner, P., 1987, Paleomagnetism and paleogeography of Mongolia in the Cretaceous, Permian and Carboniferous-preliminary data: Tectonophysics, v. 139, p. 31-39.

Rowley, D. B., 1992, Reconstructions of the Circum-Pacific, *in* Westermann, G. E. G., ed., Jurassic of the Circum-Pacific Region: Cambridge, Cambridge University Press, p. 15-26.

Rowley, D. B. , 1995, A simple geometric model for the syn-kinematic erosional denudation of thrust fronts: Earth and Planetary Science Letters, v. 129, p. 203-216.

Rowley, D.B. and Lottes, A.L., 1988, Plate kinematic reconstructions of the North Atlantic and Arctic: Late Jurassic to Present: Tectonophysics, v. 155, p. 73-120.

Rowley, D.B. and Pindell, J.L., 1989, End Paleozoic--Early Mesozoic western Pangean reconstruction and its implications for the distribution of Precambrian and Paleozoic rocks around Meso-America: Precambrian Research, v. 42, p. 411-444.

Rowley, D. B., Raymond, A., Parrish, J. T., Lottes, A. L., Scotese, C. R., and Ziegler, A. M., 1985, Carboniferous paleogeography, phytogeography, and paleoclimate reconstructions: International Journal of Coal Geology, v. 5, p. 7-42.

Sengör, A. M. C., Natal'in, B. A., and Burtman, V. S., 1993, Evolution of the Altaid tectonic collage and Palaeozoic crustal growth in Eurasia: Nature, v. 364, p. 299-307.

Shaanxi Province Bureau of Geology and Mineral Resources, 1989. Regional Geology of Shaanxi Province (in Chinese with English abstract): People's Republic of China Ministry of Geology and Mineral Resources Geological Memoirs Series 1, No. 13, 698 p.

Shaanxi Stratigraphic Group, 1983. Regional Stratigraphic Data of Northwestern China(Shaanxi) (in Chinese): Geology Press, 257 p.

Shi, G.R., 1993, Multivariate data analysis in paleoecology and paleobiogeography--a review: Palaeogeography, Palaeoclimatology, Palaeoecology, v. 105, p. 199-234.

Sichuan Province Bureau of Geology and Mineral Resources, ed., 1991, Regional Geology of Sichuan Province (in Chinese with English summary): People's Republic of China Ministry of Geology and Mineral Resources Geological Memoirs Series 1, No. 23, 730 p.

Spicer, R.A. and Parrish, J.T., 1990, Late Cretaceous--early Tertiary palaeoclimates of northern high latitudes: A quantitative view: Geological Society of London Journal, v. 147, p. 329-341.

Spicer, R.A., Rees, P.M., and Chapman, J.L., 1993, Cretaceous phytogeography and climate signals: Philosophical Transactions of the Royal Society of London B, v. 341, p. 277-284.

Stewart, W.N., 1983, Paleobotany and the Evolution of Plants: Cambridge University Press, Cambridge, 405 p.

Tang, Z., Wu, H. Y., Gao, W. L., Qin, K. L., and Liu, Y. eds., 1988, Huabei Oil Field: Petroleum Geology of China, v. 5, Beijing, Petroleum Geology of China, 569 p.

Tralau, H., 1968, Evolutionary trends in the genus Ginkgo: Lethaia, v. 1, p. 63-101.

Vakhrameev, V.A., Dobruskina, I.A., Meyen, S.V. and Zaklinskaya, E.D., 1978, Paleozoic and Mesozoic Flora of Eurasia and the Phytogeography of thoseTimes (in German): VEB Gustav Fischer Verlag Jena, 296 p.

Van der Voo, R., 1993, Paleomagnetism of the Atlantic, Tethys and Iapetus Oceans: Cambridge, Cambridge University Press, 411 p.

Walter, H., 1985, Vegetation of the Earth (3rd edition): Berlin, Springer-Verlag, 318 p.

Wang, C. L., Li, Z.J. and Xu, Q.X., 1981, The Jurassic Stratigraphic Summary of Southwestern Region: Chengdu Institute of Geology and Mineralogy, 261 p.

Wang, H. Z., 1985, Atlas of the Palaeogeography of China: Beijing, CartographicPublishing House, 85 p.

Wang, Z. W., Yang, J. L., and Gao, R. Q. eds., 1993, Daqing, Jilin Oil Field (in Chinese) Part I.: Petroleum Geology of China, v. 2, Beijing, Petroleum Industry Press, 785 p.

Wesley, A., 1973, Jurassic plants, *in* Hallam, A. Atlas of Palaeobiogeography: Elsevier, Amsterdam, p. 329-338.

Wing, S.L. and Tiffney, B.H., 1987, The reciprocal interaction of angiosperm evolution and tetrapod herbivory: Review of Palaeobotany and Palynology, v. 50, p. 179-210.

Wu, Q.Q., Hu, C.L.,Yang, W.D., Mu, Y.K. and Yu, Z. L., 1986, Biostratigraphy, lithofacies and oil and gas character of Mesozoic continental strata in Jiangsu and its neighboring districts: Nanjing Institute of Geology and Mineral Resources Bulletin Supplementary Issue 2, 100 p.

Xinjiang Stratigraphic Group, 1981, Regional Stratigraphic Data of Northwestern China(Xinjiang) (in Chinese): Geology Press, 496 p.

Zhang, M. K., Liu, D. J., Shi, Y., and Diao, Z. S., eds., 1993, Daqing, Jilin Oil Field (in Chinese) Part II. : Petroleum Geology of China, v. 2, Beijing, Petroleum Industry Press, 530 p.

Zhao, X. X., and Coe, R., 1987, Paleomagnetic constraints on the collision and rotation of North and South China: Nature, v. 327, p. 141-144.

Zhejiang Stratigraphic Group, 1979, Regional Stratigraphic Data of Eastern China(Zhejiang) (in Chinese): Geology Press, 161 p.

Ziegler, A.M., 1990, Phytogeographic patterns and continental configurations during thePermian Period, *in* McKerrow, W.S. and Scotese, C.R., eds., Palaeozoic Palaeogeography and Biogeography: Geological Society Memoir No. 12, p.363-379.

Ziegler, A.M., Parrish, J.M., Yao, J.P., Gyllenhaal, E. D., Rowley, D.B., Parrish, J.T., Nie, S.Y. Bekker, A. and Hulver, M.L., 1993, Early Mesozoic phytogeography and climate: Philosophical Transactions of the Royal Society of London B, v. 341, p. 297-305.

Ziegler, A. M., Rowley, D. B., Lottes, A. L., Sahagian, D. L., Hulver, M. L., and Gierlowski, T. C., 1985, Paleogeographic interpretation: with an example from the mid-Cretaceous, *in* Annual Reviews of Earth and Planetary Sciences, v. 13, p. 385-425.

Ziegler, A. M., Scotese, C. R., and Barrett, S., 1983, Mesozoic and Cenozoic paleogeographic maps, *in* Sündermann, B. A., ed., Tidal Friction and the Earth's Rotation II: Berlin, Springer-Verlag, p. 240-252.

Zonenshain, L.P., Kuzmin, M.I.,. and Natapoov, L.M., 1990, Geology of the U.S.S.R.: A Plate Tectonic Synthesis: Geodynamics Series v. 21, American Geophysical Union, Washington, D.C., 242 p.

Floral-data sources

Britain

Hill, C.R., Moore, D.T., Greensmith, J.T., and Williams, R., 1985, Palaeobotany and petrology of a Middle Jurassic ironstone bed at Wrack Hills, North Yorkshire: Proceedings of the Yorkshire Geological Society, v. 45, p. 277-292.

Seward, A.C., 1904, The Jurassic Flora, II. Liassic and Oolitic Floras of England: Catalogue of the Mesozoic

Plants in the Department of Geology, British Museum (Natural History), v. 4, London, 192 p.
Spicer, R.A., and Hill, C.R., 1979, Principal components and correspondence analyses of quantitative data from a Jurassic plant bed: Review of Palaeobotany and Palynology, v. 28, p. 273-299.
Van der Burgh, J., and Van Konijnenburg-Van Cittert, J.H.A., 1984, A drifted flora from theKimmeridgian (Upper Jurassic) of Lothbeg Point, Sutherland, Scotland: Review of Palaeobotany and Palynology, v. 43, p. 359-396.
Van Konijnenburg-Van Cittert, J.H.A., and Van der Burgh, J., 1989, The flora from theKimmeridgian (Upper Jurassic) of Culgower, Sutherland, Scotland: Review of Palaeobotany and Palynology, v. 61, p. 1-51.

France and Germany

Barale, G., 1981, The Jurassic paleoflora of the Jura Mountains in France: A systematicstudy of stratigraphic and paleoecological material (in French): Documents des Laboratoiresde Géologie Lyon, v. 81, 467 p.

Eastern Urals

Boyakova, V.D., and Vladimirovich, V.P., 1967, Stratigraphy of the coal measures of the Chelyabinsk basin (in Russian), in Collection of Papers on Biostratigraphy: Vsesoyuznyi Nauchno-issledovatel'skii Institut, Trudy, v. 129, p. 27-35.
Boyakova, V.D., and Yuklyaevskikh, V.V., 1967, Stratigraphy of the Lower Mesozoic deposits of the Chelyabinsk brown-coal basin (in Russian): Izvestiia Akademii Nauk SSSR,Seriia geologicheskaya, v. 4, p. 103-115.
Kiritchkova, A.I., 1961, Fossil floral complexes of the Lower Mesozoic of the eastern Urals (in Russian): Trudy VNIGRI, v. 186, p. 235-240.
Kiritchkova A.I., 1990, Triassic-Jurassic flora of the eastern Urals : Paleontologicheskii Zhurnal, v. 1, p. 69-78.
Vladimirovich, V.P., 1967, Biostratigraphy of the continental Triassic and Jurassic deposits of the eastern slope of the Urals, northern Kazakhstan and mountain area of western Siberia, *in* Martinson, G.G., ed., Stratigraphy and Paleontology of the Mesozoic and Paleogene-Neogene Continental Deposits of the Asian Part of the USSR: Leningrad, Nauka, p. 46-55.

Karatau basin, southern Kazahkstan

Doludenko, M.P. and Orlovskaya, E.R., 1975, Jurassic flora of the Karatau Ridge(southern Kazakhstan) (in Russian): Izvestiia Akademii Nauk SSSR, Seriia Geologicheskaya, v. 2, p. 121-134.

Fergana Region, eastern middle Asia, from Ghissar ridge to Issyk-Kul' depression

Doludenko, M.P. and Orlovskaya, E.R., 1975, Jurassic flora of the Karatau Ridge (southern Kazakhstan) (in Russian): Izvestiia Akademii Nauk SSSR, Seriia Geologicheskaya, v. 2, p. 121-134.
Genkina, R.Z., 1979, Subdivision of continental deposits of the Upper Triassic and Jurassic in the eastern part of the Middle Asia (in Russian): Soviet Geology, v. 4, p. 27-39.

Kuzbass

Bystritskaya ,L.I., 1974, Plant complexes in Jurassic deposits of Kuzbass (in Russian): Trudy Tomskogo Gosudarstvennogo Universiteta, v. 227, p. 32-49.
Il'ina, V.I., and Teslenko, Y.V., 1971, On the question of the boundary between the Lowerand Middle Jurassic System in continental units of Siberia (in Russian): Geology and Geophysics, v. 8, p. 3-10.
Vladimirovich, V.P., 1967, Biostratigraphy of the continental Triassic and Jurassic deposits of the eastern slope of the Urals, northern Kazakhstan and mountain area of western Siberia, *in* Martinson, G.G., ed., Stratigraphy and Paleontology of theMesozoic and Paleogene-Neogene Continental Deposits of the Asian Part of theUSSR: Leningrad, Nauka, p. 46-55.

Transbaikalia

Rasnizin, A.P., 1985, Jurassic terrestrial biocoenosis of south Siberia and surrounding territories (in Russian): Academy of Sciences of the USSR, Trudy Paleontologicheskogo Instituta, v. 213, p. 69.
Teslenko, Y.V., 1971, Materials for the study of the Toarcian flora of the eastern Transbaikal (in Rusian): Trudy SNIIGGIMS, v. 115, p. 39-42.
Teslenko, Y.V., 1975, On the stratigraphy of the Jurassic deposits of eastern Transbaikal' (in Russian): Geology and Geophysics, v. 10, p. 41-45.

South Yakutia coal basin

Markovich, E.M., 1988, Macroflora of the South Yakutiia coal basin: Newsletters in Stratigraphy, v. 19 (1/2), p.87-94.

Tarim basin

Xinjiang Stratigraphic Group, 1981, Regional Stratigraphic Data of Northwestern China (Xinjiang) (in Chinese): Beijing, Geological Publishing House, 496 p.

Ordos basin

The Institute of Geology, Chinese Academy of Geological Sciences, 1980, Mesozoic Stratigraphy and Paleontology in Shaanganning basin of China (in Chinese): Beijing, Geological Publishing House.

Nei Mongol Autonomous Region Bureau of Geology and Mineral Resources, ed., 1991, Regional Geology of Nie Mongol (Inner Mongolia) Autonomous Region (in Chinese with English summary): People's Republic of China Ministry of Geology and Mineral Resources Geological Memoirs Series 1, No. 25, 724 p.

Shaanxi Province Bureau of Geology and Mineral Resources, ed., 1989, Regional Geology of Shaanxi Province (in Chinese with English summary): People's Republic of China Ministry of Geology and Mineral Resources Geological Memoirs Series 1, No. 13, 698 p.

Sichuan basin

Editorial Group of Continental Mesozoic Stratigraphy and Paleontology in Sichuan Basin of China, 1982, Continental Mesozoic Stratigraphy and Paleontology in Sichuan Basin of China (in Chinese): Chengdu, People's Publishing House of Sichuan, 622 p.

Guizhou Province Bureau of Geology and Mineral Resources, ed., 1987, Regional Geology of Guizhou Province (in Chinese with English summary): People's Republic of China Ministry of Geology and Mineral Resources Geological Memoirs Series 1, No. 7, 698 p.

Sichuan Province Bureau of Geology and Mineral Resources, ed., 1991, Regional Geology of Sichuan Province(in Chinese with English summary): People's Republic of China Ministry of Geology and Mineral Resources Geological Memoirs Series 1, No. 23, 730 p.

Fujian

Bureau of Geology and Mineral Resources of Fujian Province, ed., 1985, Regional Geology of Fujian Province (in Chinese with English summary): People's Republic of China Ministry of Geology and Mineral Resources Geological Memoirs Series 1, Number 4, 671 p.

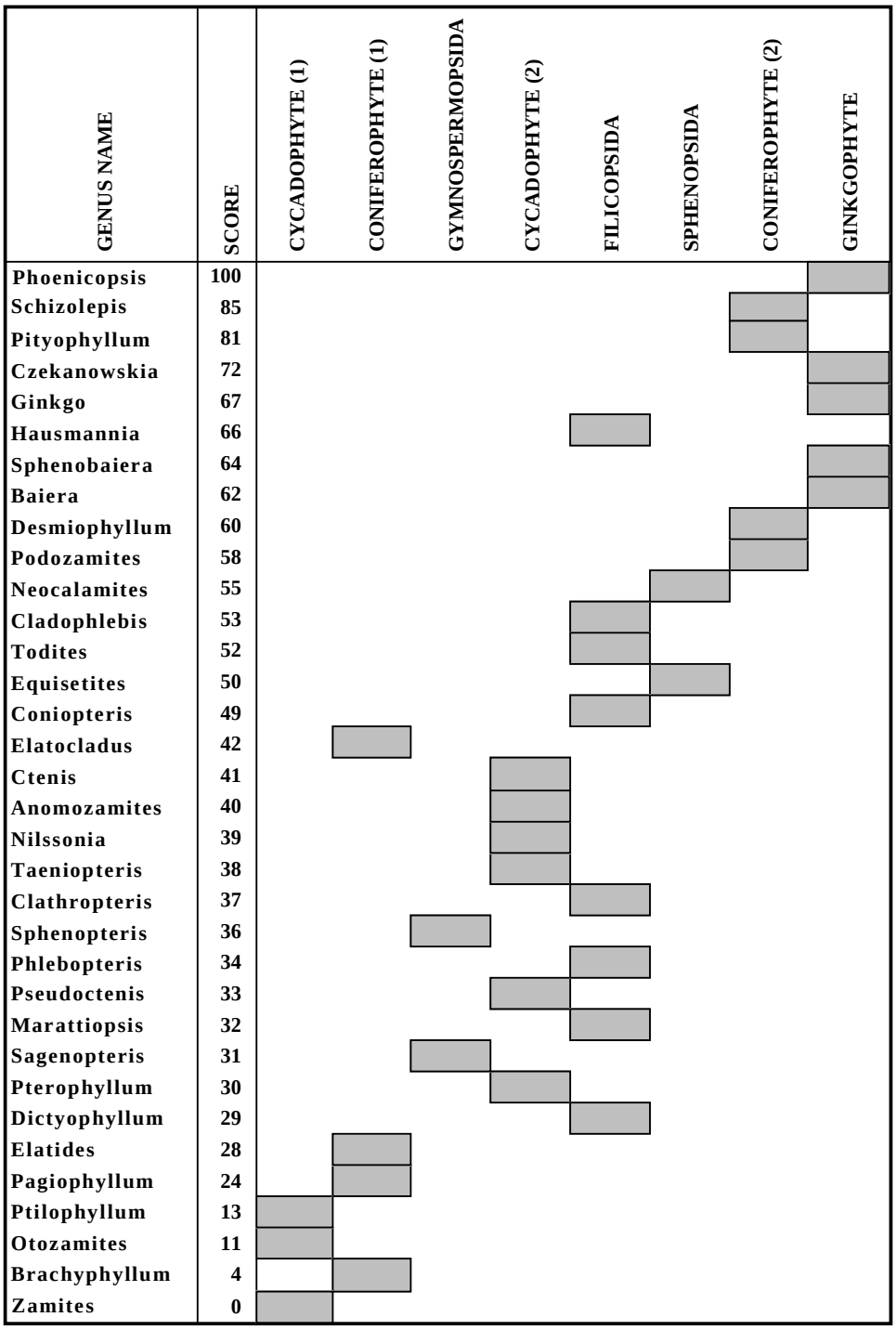

Figure 17.1. Gradient scores and taxonomic affinities of the 34 most common plant genera. The scores were derived from the early to middle Jurassic axis-1 correlation (Ziegler et al., 1993, fig. 1). Cycadophytes (1) and (2) stand for Cycadales and Bennettitales with narrow and broad leaflets, respectively. Coniferophytes (1) and (2) stand for microphyllous versus broad-leaved deciduous types, respectively. The Filicopsida and the Spenopsida are the groups in which the modern ferns and horsetails are classified, respectively, while the ginkgophyte category contains *Ginkgo* and numerous more or less related forms.

Mesozoic assembly of Asia (Ziegler et al., 1996)

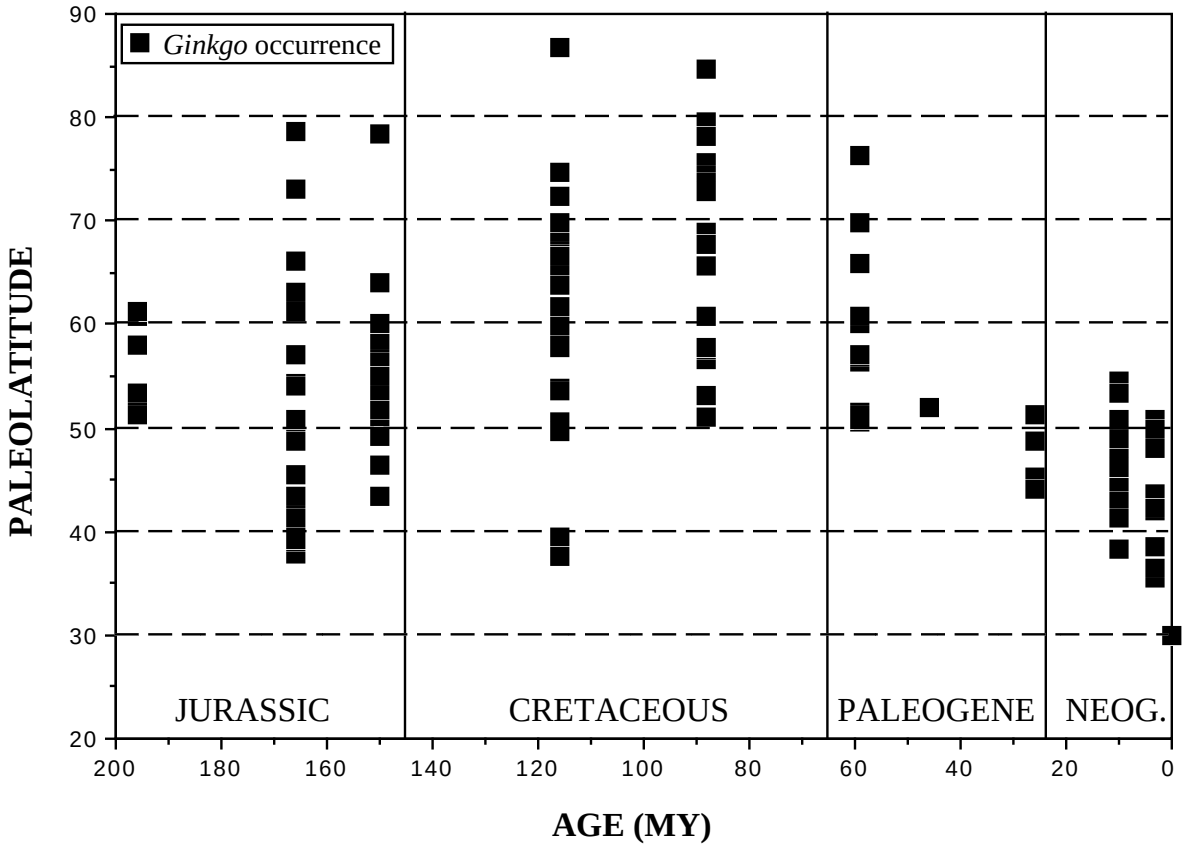

Figure 17.2. Paleo-latitudinal occurrence of the genus *Ginkgo* from the Jurassic to the present. The data are mainly from Tralau (1968) and have been supplemented by data from Del Tredici et al. (1992), Wang et al. (1981), Wu et al. (1986), Bureau of Geology and Mineral Resources of Jilin Province (1988), and the provincial Hebei, Heilongjiang, Jilin, Liaoning, Ningxia, Shaanxi, Xinjiang, and Zhejiang stratigraphic groups in the Regional Stratigraphic Data series.

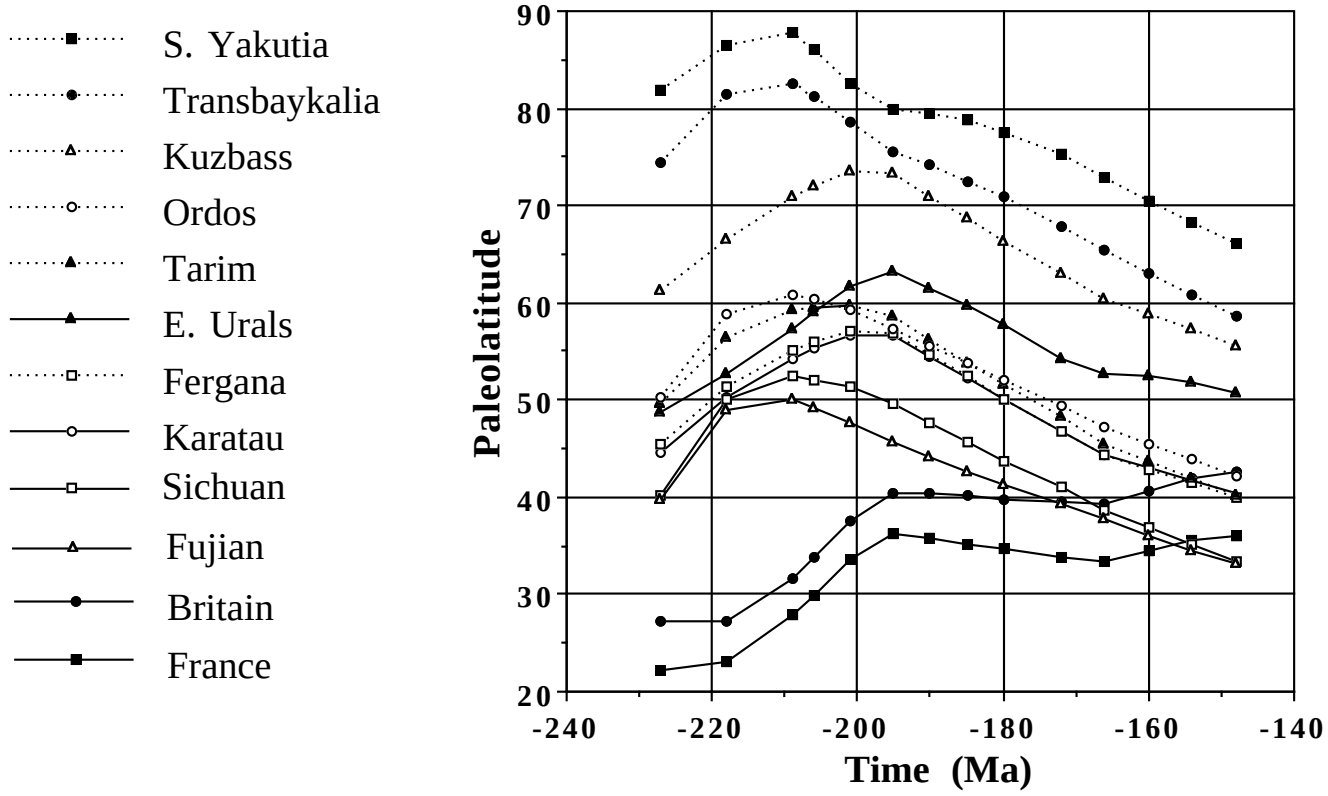

Figure 17.3. Paleo-latitudinal paths through the late Triassic and Jurassic for the 12 sampled basins. Northern Eurasian paths are derived from globally constrained plate-motion data. The Chinese microcontinent paths are less certain and are reconstructed from our knowledge of their tectonic relationships with northern Eurasia. There is one symbol for each stage, whether or not that stage was sampled for that basin.

Figure 17.4 Mesozoic assembly of Asia (Ziegler et al., 1996)

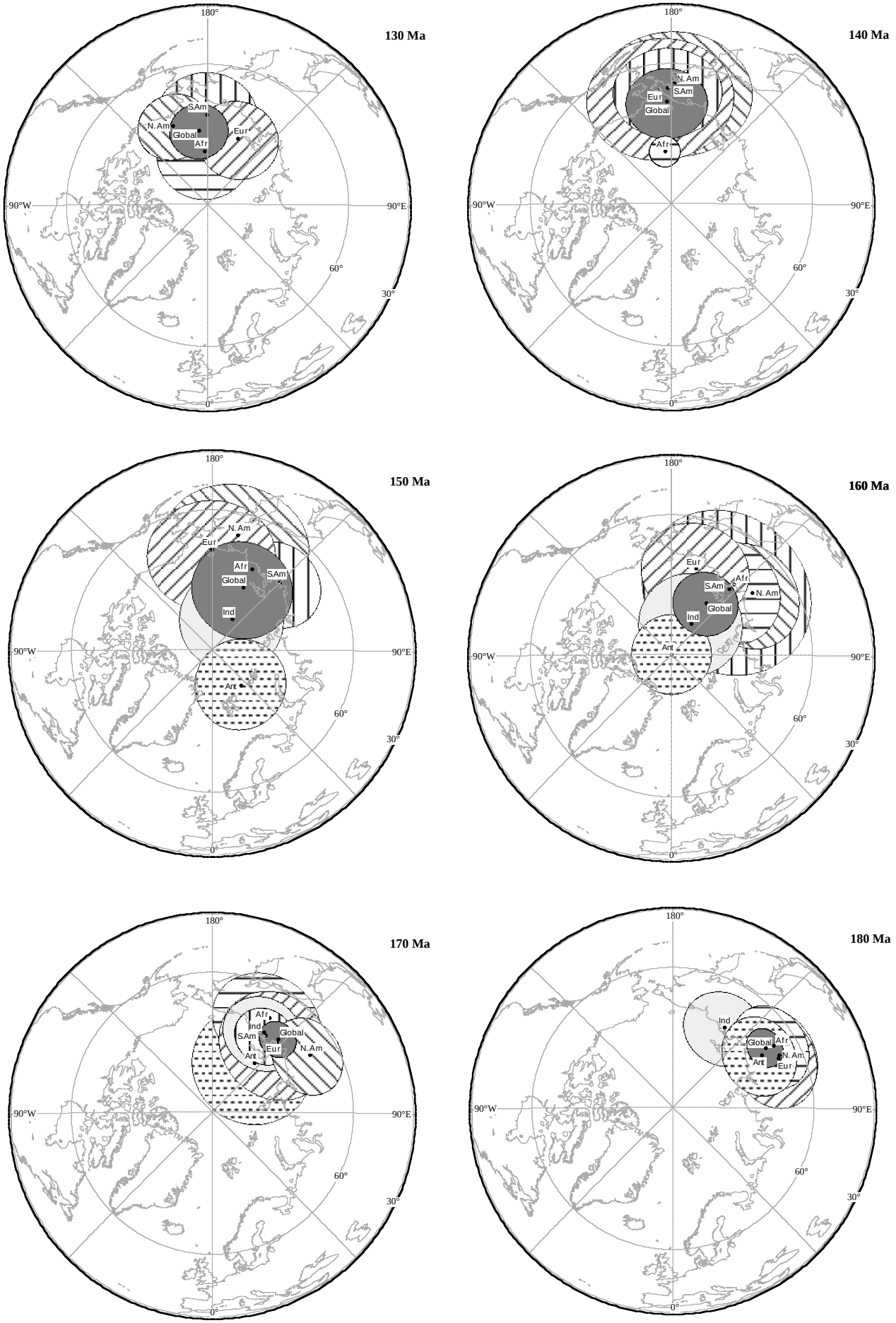

Figure 17.4 (contd.)

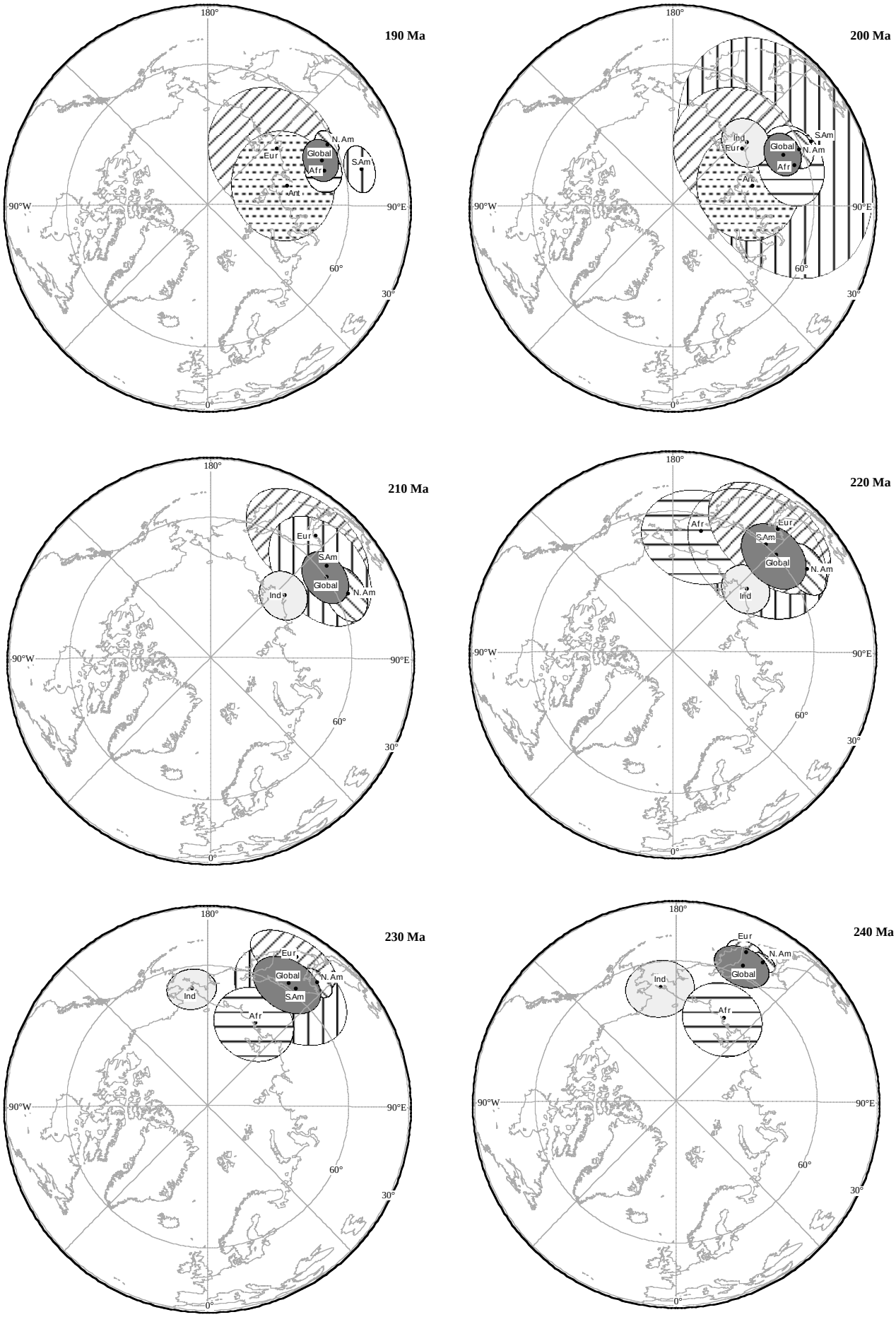

Figure 17.4 (contd.)

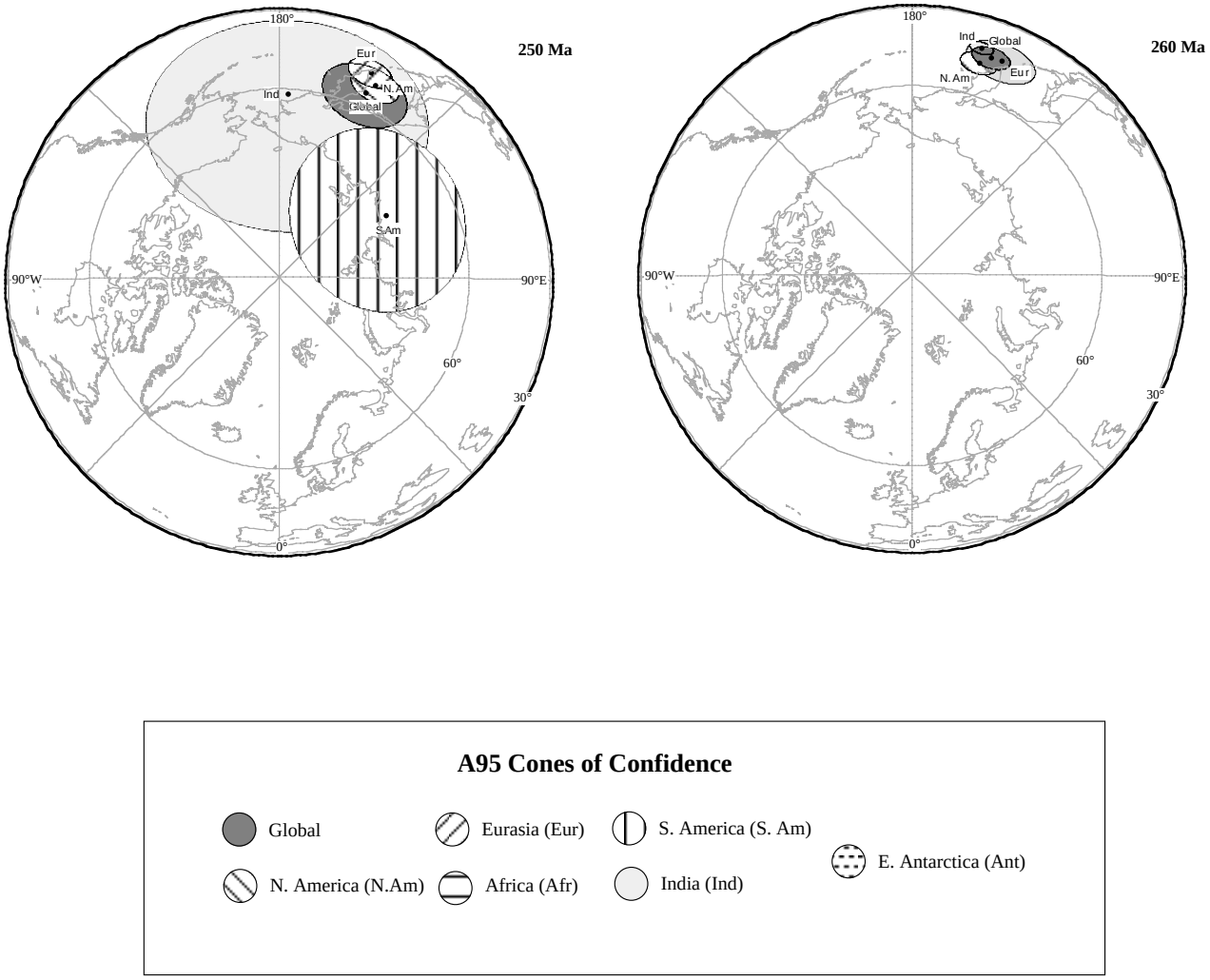

Figure 17.4. Polar orthographic maps of the continental interval means and A95 for North America, Eurasia, Africa, South America, India, and Eastern Antarctica in Eurasian fixed coordinates. The poles from which these maps are derived are listed in Table 17.2, rotated using rotation parameters derivable from Table 17.3. The means and their associated statistics are listed in Table 17.4. The global mean pole that is plotted is the weight interval mean of Table 17.4.

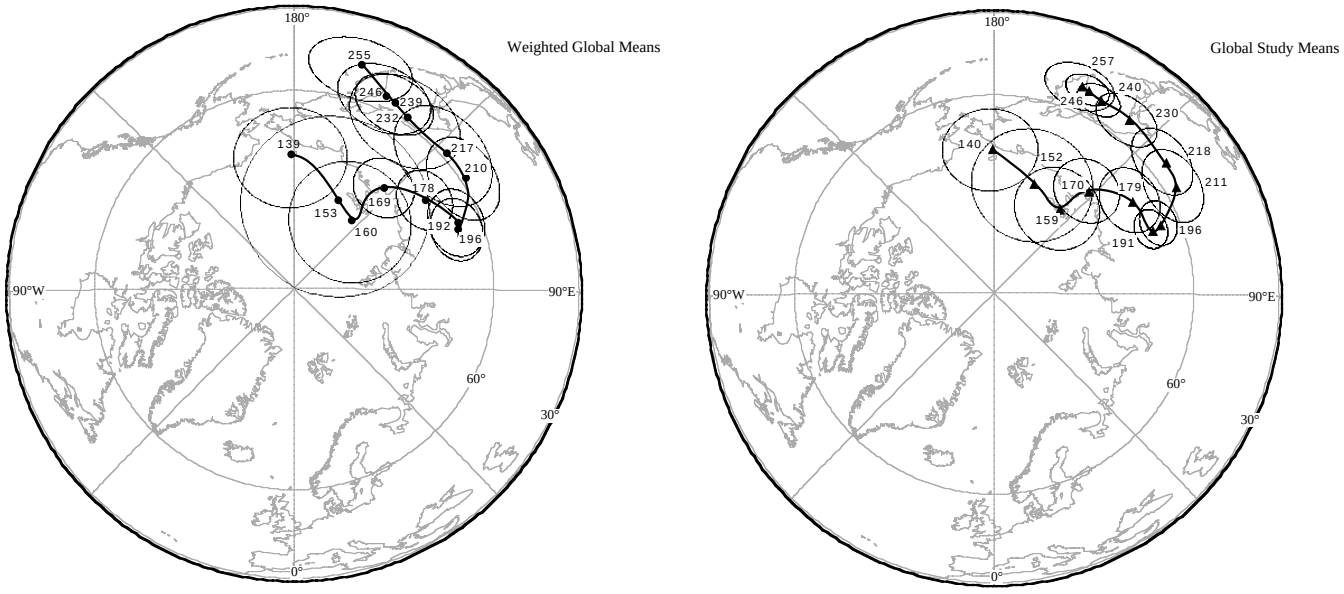

Figure 17.5a. Global weighted mean APWP and associated A95 values for the interval from the late Permian to the early Cretaceous in Eurasian fixed coordinates. (b). Global study mean path and associated A95 values for the interval from the same interval in Eurasian fixed coordinates.

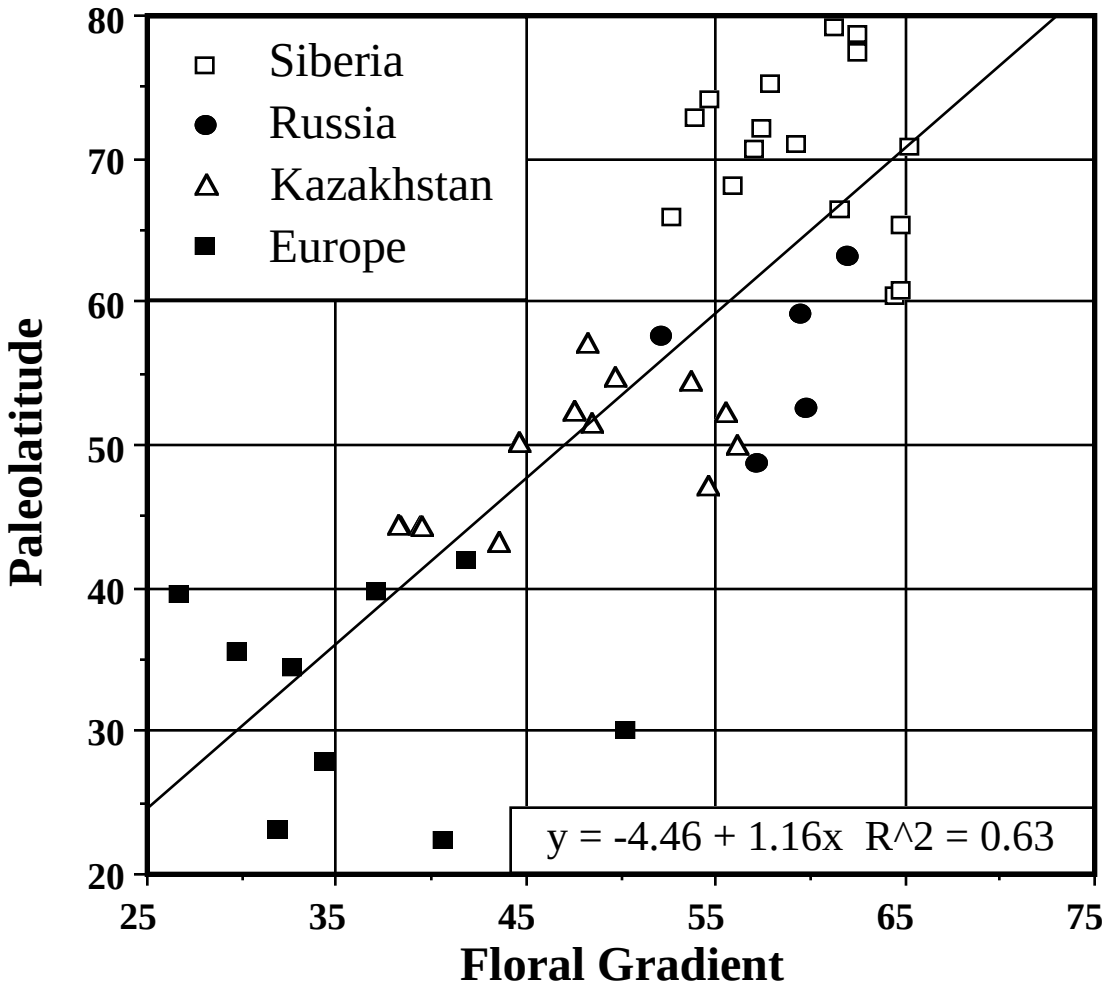

Figure 17.6. Correlation of the floral-gradient scores (from Table 17.1) for the northern Eurasian basins with paleo-latitude (from Figure 17.3). Siberia includes the data from Kuzbass, Transbaikalia, and South Yakutia basins; Kazakhstan includes Karatau and Fergana; Russia consists of the eastern Urals; Europe includes Britain and France/Germany.

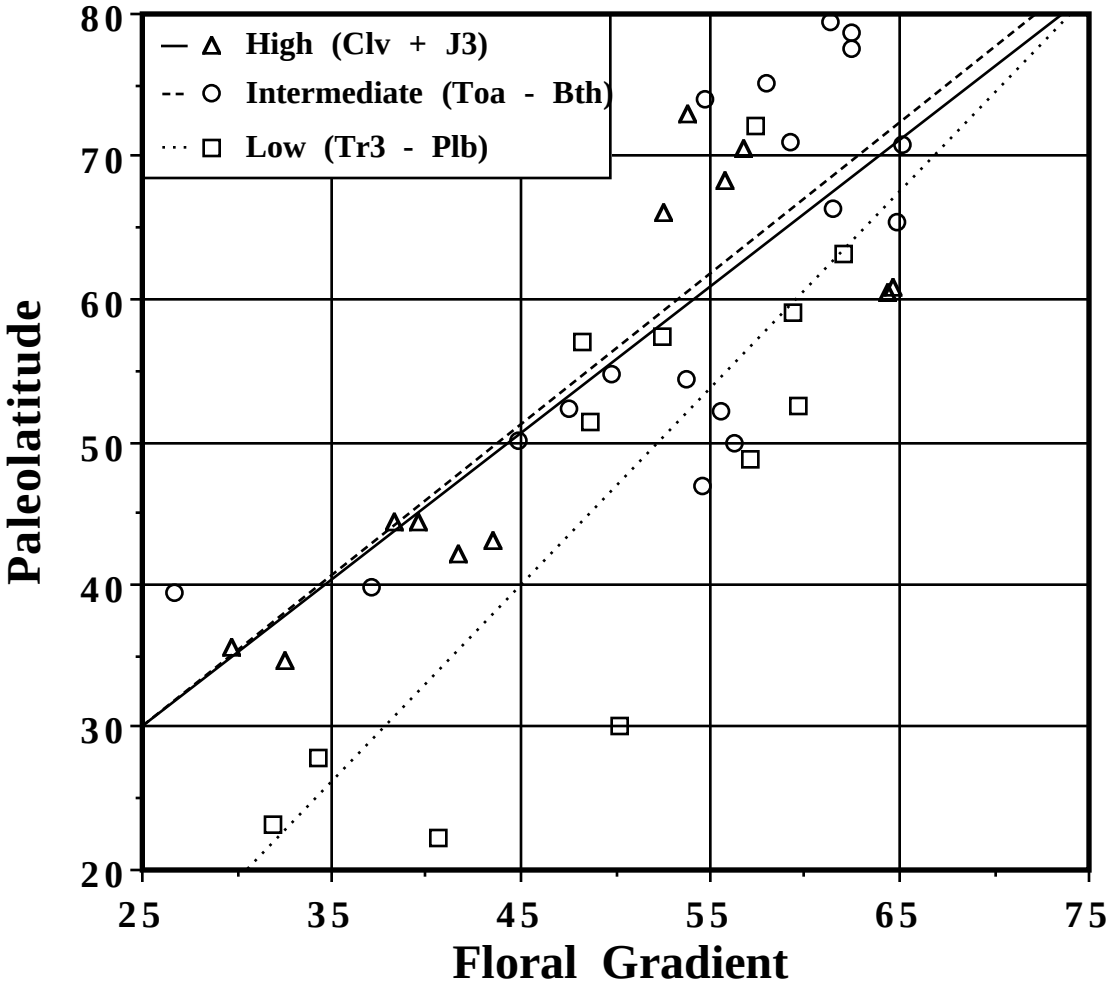

Figure 17.7. Correlation of the floral-gradient scores with paleo-latitude, as in Figure 17.4, but with individual symbols and lines according to sea level. The low-sea-level intervals range from the late Triassic through the Pliensbachian stage of the early Jurassic. The intermediate-sea-level intervals range from the Toarcian stage through the Bathonian stage of the middle Jurassic, and the high-sea-level stage includes the Callovian stage to the end of the period.

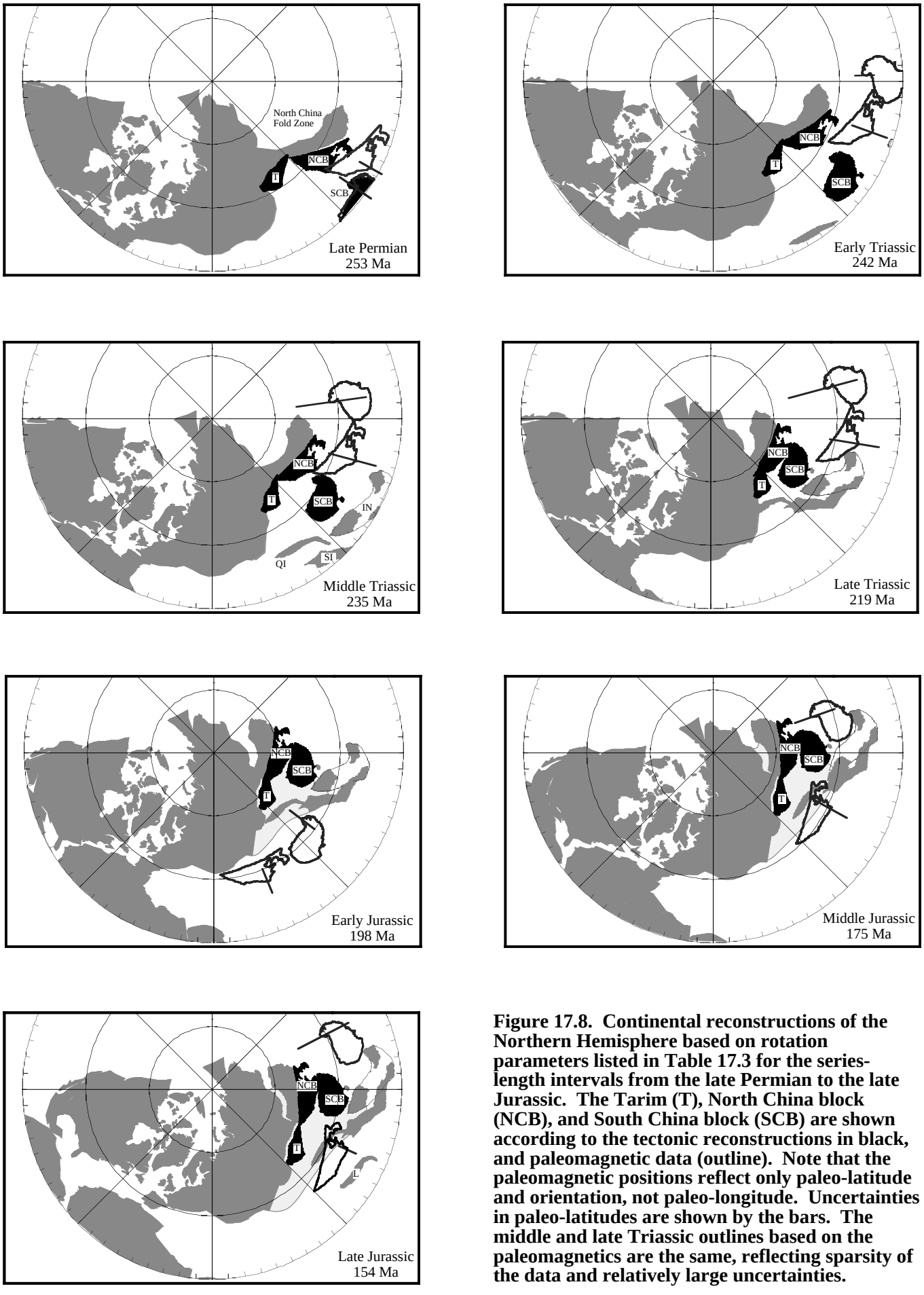

Figure 17.8. Continental reconstructions of the Northern Hemisphere based on rotation parameters listed in Table 17.3 for the series-length intervals from the late Permian to the late Jurassic. The Tarim (T), North China block (NCB), and South China block (SCB) are shown according to the tectonic reconstructions in black, and paleomagnetic data (outline). Note that the paleomagnetic positions reflect only paleo-latitude and orientation, not paleo-longitude. Uncertainties in paleo-latitudes are shown by the bars. The middle and late Triassic outlines based on the paleomagnetics are the same, reflecting sparsity of the data and relatively large uncertainties.

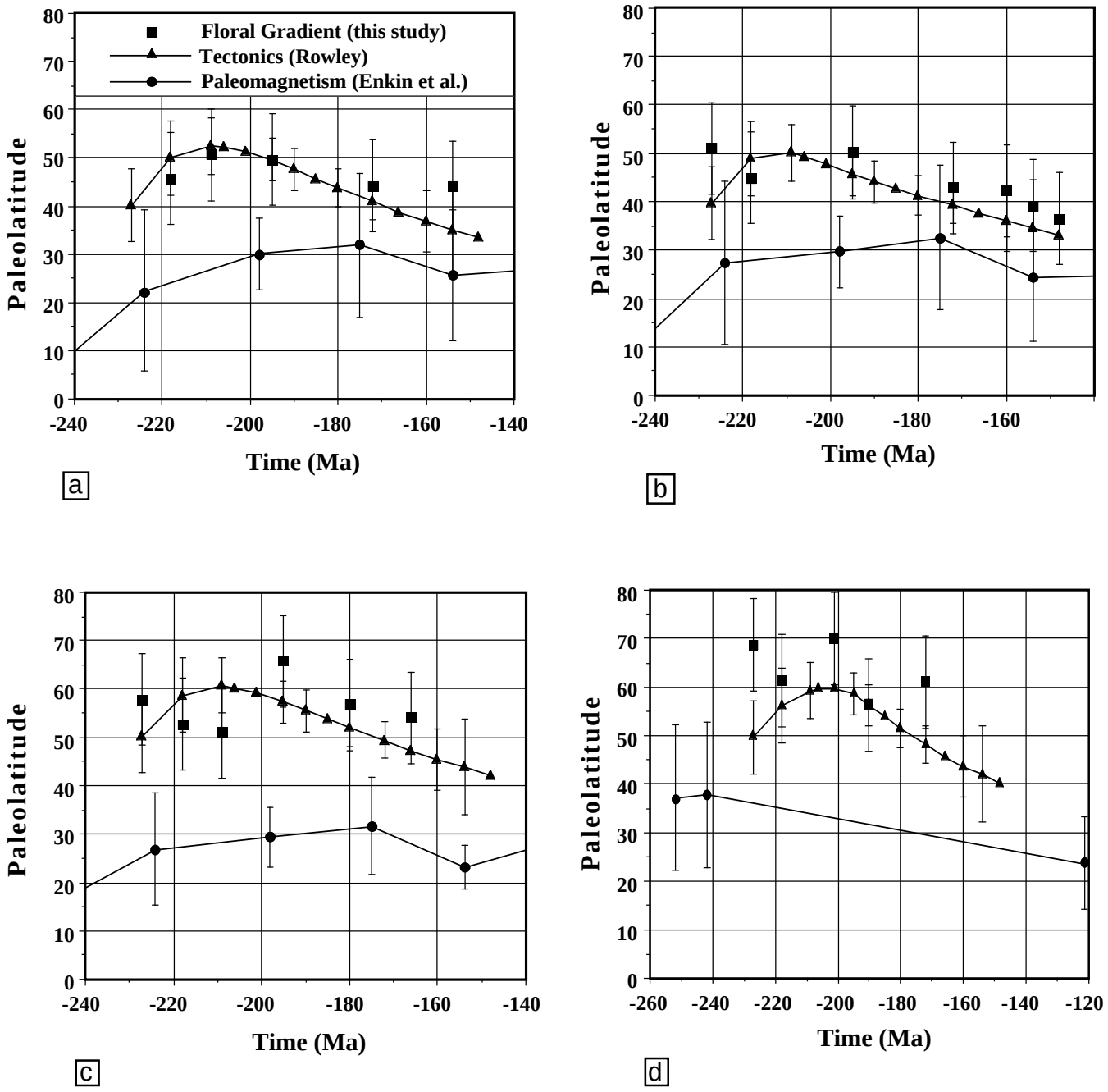

Figure 17.9. Paleo-latitudinal estimates for the Sichuan basin (a) and Fujian basin (b) of South China, the Ordos basin (c) of North China, and the Tarim basin (d), based on paleomagnetism, tectonics, and the floral-gradient scores. Error bars are one standard deviation on either side of the regression line (Figure 17.6) on the Enkin et al. (1992) APWP, and on the tectonically constrained position the errors are equal to the A95 values.

Table 17.1. Floral data collated for this study, shown stage by stage for each basin.

		BRITAIN (55, -1)[a]			FRANCE/ GERMANY (48, 5)						EAST URALS (55, 61)					KARATAU (42, 70)					FERGANA REGION (41, 73)							KUZBASS (54, 88)				TRANSBAYK. (51, 116)			
Genus	**Score[b]**	**Bj[c]**	**Bt**	**Ki**	**Cn**	**No**	**Rh**	**He**	**Ox**	**Ki**	**Cn**	**No**	**Rh**	**He**	**Pl**	**To**	**Aa**	**Bj**	**Ca**	**Ox**	**No**	**Si**	**To**	**Aa**	**Bj**	**Bt**	**Ca**	**He**	**To**	**Bj**	**Ca**	**To**	**Bj**	**Ca**	**Ki**
Phoenicopsis	100			x								x	x	x	x	x	x	x		x	x	x	x	x	x	x		x	x	x	x	x	x	x	x
Schizolepis	85							x														x	x	x		x			x	x	x				
Pityophyllum	81													x		x	x	x	x	x	x	x	x	x	x	x	x	x	x	x	x	x	x		
Czekanowskia	72	x		x							x		x	x	x	x	x		x	x	x	x	x	x	x	x	x	x	x	x	x	x	x		x
Ginkgo	67		x	x							x	x		x							x	x	x	x	x	x	x	x	x	x	x				
Hausmannia	66			x				x												x	x	x		x	x			x				x				
Sphenobaiera	64	x			x			x			x	x	x	x		x		x		x	x	x	x	x	x	x		x	x	x			x	x	x
Baiera	62	x		x				x	x	x	x			x		x	x			x	x	x	x	x	x	x		x	x						
Desmiophyllum	60																																x		
Podozamites	58			x				x			x	x	x	x		x	x			x	x	x	x	x	x	x	x	x	x	x		x	x	x	
Neocalamites	55	x			x			x				x	x	x		x	x	x			x	x	x	x	x			x	x						
Cladophlebis	53	x		x			x		x	x	x	x	x	x	x	x	x	x	x	x	x	x	x	x	x	x	x	x	x	x	x	x	x	x	x
Todites	52			x				x			x	x										x		x					x						
Equisetites	50	x		x	x	x	x	x				x				x	x	x		x	x	x	x	x	x	x	x	x	x	x		x	x		x
Coniopteris	49	x		x					x					x	x	x	x	x		x			x	x	x	x	x	x	x	x	x	x	x	x	x
Elatocladus	42	x		x													x		x	x			x	x	x	x	x			x		x			
Ctenis	41	x																			x	x	x	x	x	x	x					x			
Anomozamites	40												x			x	x				x	x	x	x	x	x		x		x					
Nilssonia	39	x		x		x										x	x	x	x	x		x	x	x	x	x	x			x		x			
Taeniopteris	38					x	x					x	x	x		x	x	x		x	x	x	x	x	x	x									
Clathropteris	37	x			x	x	x	x					x	x		x	x			x	x	x	x	x	x	x		x	x						
Sphenopteris	36		x	x	x				x	x				x	x					x								x				x			
Phlebopteris	34	x	x	x				x													x	x	x	x	x	x			x						
Pseudoctenis	33	x		x												x		x	x			x	x	x	x										
Marattiopsis	32	x		x																		x	x	x	x	x									
Sagenopteris	31	x	x	x				x											x	x			x	x	x	x									
Pterophyllum	30			x	x	x		x					x			x			x	x	x	x	x	x	x	x		x							
Dictyophyllum	29	x	x		x	x		x			x		x								x	x	x												
Elatides	28	x		x																	x			x	x	x		x	x						
Pagiophyllum	24				x		x		x	x										x		x	x	x	x	x						x			
Ptilophyllum	13	x	x	x																x				x	x	x	x								
Otozamites	11	x		x															x	x	x	x			x	x	x								
Brachyphyllum	4	x	x	x			x		x	x									x	x	x	x		x	x	x	x								
Zamites	0	x	x	x		x			x	x										x							x								
Avge. score/ locality		37	27	42	41	32	34	50	33	30	57	60	52	59	62	54	55	56	40	44	49	48	50	48	45	46	38	57	59	62	64	55	65	#	65

[a]Present latitude and longitude for each basin.

[b]Floral-gradient score, with the average score for each composite list given at the bottom.

[c]Carnian (Cn), Norian (No), Rhaetic (Rh), Hettangian (He), Sinemurian (Si), Pliensbachian (Pl), Toarcian (To), Aalenian (Aa), Bajocian (Bj), Bathonian (Ba), Callovian (Ca), Oxfordian (Ox), Kimmeridgian (Ki), and Volgian (Vo).

***Source*: Data sources for each basin are given at the end of the References section.**

Table 17.1. (contd.)

		SOUTH YAKUTIA (57, 125)								TARIM (40, 85)					ORDOS BASIN (37, 110)						SICHUAN (31, 106)					FUJIAN (26, 118)						
Genus	**Score**	**To**	**Aa**	**B j**	**Bt**	**Ca**	**Ox**	**K i**	**Vo**	**Cn**	**No**	**S i**	**To**	**Bt**	**Cn**	**No**	**R h**	**P l**	**B j**	**Ca**	**No**	**R h**	**P l**	**Bt**	**K i**	**Cn**	**No**	**P l**	**Bt**	**Ox**	**K i**	**Vo**
Phoenicopsis	100	x	x	x	x	x	x	x	x	x	x	x	x	x				x	x	x								x		x	x	
Schizolepis	85	x	x	x	x	x	x	x	x											x		x	x									
Pityophyllum	81	x	x	x	x	x	x	x	x	x	x	x	x	x				x		x	x	x	x									
Czekanowskia	72	x	x	x	x	x	x	x	x	x		x	x	x				x	x	x	x	x	x					x				
Ginkgo	67	x	x	x	x	x	x	x	x	x		x	x	x	x	x	x	x	x	x	x	x						x				
Hausmannia	66					x	x	x	x		x							x	x	x	x	x	x				x	x				
Sphenobaiera	64	x	x	x	x	x	x	x	x		x		x		x			x	x	x	x	x	x			x	x	x			x	x
Baiera	62			x				x	x	x			x	x			x	x	x		x	x	x	x		x	x	x			x	
Desmiophyllum	60													x	x		x	x		x		x	x			x						
Podozamites	58	x					x		x	x	x	x	x	x	x	x	x	x	x	x	x	x	x	x	x	x	x	x	x	x		x
Neocalamites	55	x								x	x		x		x	x	x		x	x	x	x	x	x		x	x	x		x		
Cladophlebis	53	x	x	x	x	x	x	x	x	x	x	x	x	x	x	x	x		x	x	x	x	x	x		x	x	x	x	x	x	x
Todites	52	x								x	x		x	x	x	x	x	x	x	x	x	x	x			x	x	x	x			
Equisetites	50	x	x	x	x	x	x	x	x				x	x			x				x	x	x	x		x	x	x	x	x		
Coniopteris	49	x	x	x	x	x	x	x	x		x	x	x	x				x	x	x			x	x	x			x	x	x		x
Elatocladus	42				x	x	x	x	x									x	x	x	x	x	x		x		x	x		x		x
Ctenis	41								x				x							x	x	x	x			x	x					
Anomozamites	40												x	x			x		x	x	x	x	x			x	x			x		x
Nilssonia	39					x		x	x				x	x	x		x		x		x	x	x	x		x	x	x			x	x
Taeniopteris	38		x	x	x	x	x	x	x				x				x			x	x	x	x			x	x	x				
Clathropteris	37										x		x								x	x	x				x	x				
Sphenopteris	36										x		x	x	x		x	x	x	x	x	x	x		x					x		x
Phlebopteris	34	x										x						x			x		x				x	x				
Pseudoctenis	33																			x	x	x	x									
Marattiopsis	32									x									x		x		x				x					
Sagenopteris	31																x			x	x	x					x	x		x	x	x
Pterophyllum	30							x	x					x			x				x	x	x	x		x	x	x				x
Dictyophyllum	29										x										x	x	x			x	x	x				
Elatides	28	x	x	x	x	x		x	x																							
Pagiophyllum	24				x	x	x	x	x											x					x					x		x
Ptilophyllum	13																				x	x	x	x					x	x	x	x
Otozamites	11															x			x	x	x		x	x				x	x	x	x	x
Brachyphyllum	4					x	x		x				x							x										x	x	x
Zamites	0																				x	x					x	x			x	
Avge. score/ locality		61	63	62	58	54	57	56	53	63	57	64	53	57	54	49	48	60	53	51	43	48	47	42	42	48	43	47	41	40	38	35

Table 17.2. Paleomagnetic poles[a]

Plate Name	Pole number	Average age of magnetization[b]	Block name[c]	Eurasian Coordinates						
				Age (Ma)	Lat. (°N)	Long. (°E)	Age (Ma)	Lat. (°N)	Long. (°E)	A95 (°)
N. America	A1.033	120	N. America	130	68	-134				3
N. America	A1.034	121	N. America	130	73	174				18
N. America	A1.036	127	N. America	130	76	-165				2
N. America	A1.037	129	N. America	130	73	-132				4
N. America	A1.038	130	N. America	130	68	-162	140	68	-160	14
N. America	A1.039	147	Colorado Plat.	140	66	177	150	66	179	4
N. America	A1.040	149	Colorado Plat.	140	57	163	150	57	164	5
N. America	A1.043	152	N. America	150	74	151	160	74	153	11
N. America	A1.045	165	N. America	160	65	116	170	65	117	11
N. America	A1.046	165	Colorado Plat.	160	62	137	170	62	139	4
N. America	A1.047	169	N. America	160	74	103	170	74	105	7
N. America	A1.051	179	N. America	170	71	104	180	71	105	1
N. America	A1.052	179	N. America	170	61	123	180	62	125	1
N. America	A1.053	190	N. America	190	69	111	200	70	114	11
N. America	A1.054	189	N. America	180	63	116	190	64	118	8
N. America	A1.056	194	N. America	190	59	116	200	60	117	2
N. America	A1.057	194	N. America	190	61	132	200	61	134	4
N. America	A1.059	194	N. America	190	61	113	200	62	114	11
N. America	A1.060	193	N. America	190	62	111	200	63	113	3
N. America	A1.061	195	N. America	190	59	109	200	60	111	2
N. America	A1.062	196	Colorado Plat.	190	57	120	200	58	121	10
N. America	A1.063	196	Colorado Plat.	190	58	113	200	59	114	7
N. America	A1.064	197	N. America	190	63	97	200	63	98	11
N. America	A1.065	211	N. America	210	60	120	220	61	122	3
N. America	A1.066	202	Colorado Plat.	200	56	93	210	57	94	5
N. America	A1.068	201	Cordillera FTB	200	55	94	210	56	95	8
N. America	A1.069	200	N. America	200	60	132	210	61	134	2
N. America	A1.070	196	N. America	190	51	115	200	52	117	11
N. America	A1.071	206	N. America	200	53	124	210	53	125	5
N. America	A1.072	212	N. America	210	48	82	220	49	83	13
N. America	A1.073	215	N. America	210	58	119	220	59	121	5
N. America	A1.074	212	N. America	210	61	143	220	62	146	11
N. America	A1.075	214	Cordillera FTB	210	58	96	220	59	97	4
N. America	A1.076	214	N. America	210	56	110	220	56	111	4
N. America	A1.077	219	N. America	210	53	132	220	53	134	5
N. America	A1.078	219	N. America	210	47	120	220	48	122	5
N. America	A1.080	221	N. America	220	44	130	230	45	132	7
N. America	A1.081	221	N. America	220	47	125	230	48	126	4
N. America	A1.082	226	Colorado Plat.	220	59	131	230	59	133	3
N. America	A1.083	230	Front Range	230	56	130	240	56	132	14
N. America	A1.084	228	N. America	220	47	132	230	48	133	3
N. America	A1.085	235	N. America	230	58	134	240	58	136	3
N. America	A1.087	240	Colorado Plat.	240	56	134	250	57	136	5
N. America	A1.088	240	Colorado Plat.	240	53	148	250	54	150	3
N. America	A1.089	240	Colorado Plat.	240	55	145	250	56	147	6
N. America	A1.090	240	Colorado Plat.	240	56	146	250	57	148	2
N. America	A1.092	235	Front Range	230	49	139	240	49	141	5
N. America	A1.093	241	Front Range	240	47	157	250	47	159	7
N. America	A1.094	237	Front Range	230	47	148	240	48	150	2
N. America	A1.095	237	Front Range	230	45	150	240	46	151	4
N. America	A1.096	246	N. America	240	52	147	250	52	149	0
N. America	A1.097	249	N. America	240	56	155	250	56	157	15
N. America	A1.098	251	Colorado Plat.	250	51	158	260	51	158	8
N. America	A1.099	258	N. America	250	52	164	260	52	164	5
N. America	A1.100	250	N. America	250	52	165	260	52	165	5
Eurasia	A2.037	141	Eurasia	140	75	179	150	75	179	3
Eurasia	A2.039	128	Eurasia	130	76	155				8
Eurasia	A2.040	149	Svalbard	140	66	-159	150	66	-159	4
Eurasia	A2.041	150	Svalbard	150	58	-179	160	58	-179	9
Eurasia	A2.044	156	Eurasia	150	78	148	160	78	148	6
Eurasia	A2.046	164	Eurasia	160	74	-160	170	74	-160	4
Eurasia	A2.047	162	Eurasia	160	72	150	170	72	150	7
Eurasia	A2.049	172	Eurasia	170	63	117	180	63	117	2
Eurasia	A2.051	178	Eurasia	170	63	120	180	63	120	6
Eurasia	A2.053	190	Eurasia	190	73	105	200	73	105	4
Eurasia	A2.054	195	Eurasia	190	77	135	200	77	135	2
Eurasia	A2.058	219	Eurasia	210	44	134	220	44	134	0
Eurasia	A2.059	219	Eurasia	210	48	157	220	48	157	7
Eurasia	A2.061	217	Eurasia	210	44	110	220	44	110	4
Eurasia	A2.063	237	Eurasia	230	49	146	240	49	146	15
Eurasia	A2.064	237	Eurasia	230	48	153	240	48	153	13
Eurasia	A2.065	240	Eurasia	240	60	127	250	60	127	2
Eurasia	A2.066	242	Eurasia	240	59	146	250	59	146	7
Eurasia	A2.067	240	Eurasia	240	48	138	250	48	138	0
Eurasia	A2.068	242	Eurasia	240	52	167	250	52	167	10

Plate Name	Pole number	Average age of magnetization[b]	Block name[c]	Eurasian Coordinates						
				Age (Ma)	Lat. (°N)	Long. (°E)	Age (Ma)	Lat. (°N)	Long. (°E)	A95 (°)
Eurasia	A2.069	242	Eurasia	240	49	159	250	49	159	11
Eurasia	A2.070	242	Eurasia	240	52	165	250	52	165	4
Eurasia	A2.071	242	Eurasia	240	52	145	250	52	145	3
Eurasia	A2.072	242	Eurasia	240	56	146	250	56	146	12
Eurasia	A2.073	242	Eurasia	240	51	151	250	51	151	1
Eurasia	A2.074	242	Eurasia	240	43	146	250	43	146	5
Eurasia	A2.075	242	Eurasia	240	53	158	250	53	158	4
Eurasia	A2.077	251	Eurasia	250	51	161	260	51	161	4
Eurasia	A2.078	256	Eurasia	250	50	143	260	50	143	4
Eurasia	A2.079	256	Eurasia	250	52	144	260	52	144	3
Eurasia	A2.081	247	Eurasia	240	51	166	250	51	166	4
Eurasia	A2.082	250	Eurasia	250	43	169	260	43	169	2
Eurasia	A2.083	255	Eurasia	250	47	171	260	47	171	6
Eurasia	A2.085	263	Eurasia	260	47	156				5
Eurasia	A2.086	263	Eurasia	260	49	154				1
Africa	A4.I.029	130	S. Africa	130	80	-175	140	80	-178	3
Africa	A4.I.030	120	Morocco	130	71	-161				15
Africa	A4.I.032	125	E. Africa	130	78	116				9
Africa	A4.I.033	129	S. Africa	130	82	-167				10
Africa	A4.I.036	155	S. Africa	150	69	-120	160	68	-131	6
Africa	A4.I.037	156	West Africa	150	54	117	160	52	116	6
Africa	A4.I.038	160	West Africa	160	68	134	170	65	131	19
Africa	A4.I.039	167	S. Africa	160	70	121	170	67	119	7
Africa	A4.I.040	168	S. Africa	160	79	137	170	76	133	11
Africa	A4.I.041	173	West Africa	170	61	172	180	61	169	9
Africa	A4.I.042	173	Morocco	170	60	168	180	59	165	11
Africa	A4.I.043	180	West Africa	180	69	113	190	69	115	14
Africa	A4.I.044	180	West Africa	180	65	131	190	65	133	6
Africa	A4.I.045	182	West Africa	180	64	115	190	65	117	4
Africa	A4.I.046	183	West Africa	180	59	91	190	59	92	7
Africa	A4.I.047	187	West Africa	180	60	115	190	61	116	4
Africa	A4.I.048	187	West Africa	180	63	111	190	64	112	6
Africa	A4.I.049	189	S. Africa	180	69	78	190	70	79	9
Africa	A4.I.051	193	S. Africa	190	66	90	200	67	91	15
Africa	A4.I.052	193	S. Africa	190	65	109	200	66	111	13
Africa	A4.I.053	193	S. Africa	190	72	127	200	72	130	8
Africa	A4.I.056	196	Morocco	190	56	109	200	56	111	7
Africa	A4.I.057	206	S. Africa	200	56	108	210	56	109	5
Africa	A4.I.059	219	Morocco	210	64	163	220	65	166	12
Africa	A4.I.066	235	S. Africa	230	71	148	240	71	151	8
S. America	A4.II.118	121	S. America	130	72	172				10
S. America	A4.II.119	129	S. America	130	83	153				4
S. America	A4.II.120	123	S. America	130	66	-168				6
S. America	A4.II.123	139	S. America	140	69	176	150	70	173	11
S. America	A4.II.125	158	S. America	150	73	135	160	70	135	9
S. America	A4.II.127	166	Patagonia	160	75	143	170	72	138	6
S. America	A4.II.131	199	S. America	190	54	103	200	55	104	5
S. America	A4.II.132	204	Patagonia	210	58	128	220	57	127	13
S. America	A4.II.133	220	Patagonia	220	49	136	230	49	138	10
S. America	A4.II.134	224	Patagonia	220	66	130	230	67	132	14
S. America	A4.II.135	227	S. America	220	63	149	230	63	152	10
S. America	A4.II.136	232	Patagonia	230	676	125	240	67	127	13
S. America	A4.II.145	237	S. America	240	45	159	250	44	157	12
S. America	A4.II.147	256	S. America	250	72	120	260	72	120	14
S. America	A4.II.150	263	Patagonia	260	56	160				12
S. America	A4.II.151	266	S. America	260	63	159				3
S. America	A4.II.152	266	S. America	260	67	129				3
E. Antarctica	A5.II.027	155	E. Antarctica	150	75	49	160	79	72	3
E. Antarctica	A5.II.028	158	E. Antarctica	150	81	29	160	86	74	10
E. Antarctica	A5.II.029	155	E. Antarctica	150	77	6	160	83	9	2
E. Antarctica	A5.II.030	179	E. Antarctica	170	73	124	180	71	124	3
E. Antarctica	A5.II.031	164	E. Antarctica	160	90	-81	170	85	170	4
E. Antarctica	A5.II.032	165	E. Antarctica	160	81	-146	170	77	-166	5
E. Antarctica	A5.II.033	195	E. Antarctica	190	70	81	200	70	82	7
E. Antarctica	A5.II.034	195	E. Antarctica	190	74	116	200	75	118	4
E. Antarctica	A5.II.035	195	E. Antarctica	190	76	120	200	76	122	5
India	A5.IV.137	175	India	170	73	152	180	71	148	8
India	A5.IV.138	211	India	210	71	131	220	72	133	5
India	A5.IV.140	237	India	230	66	-175	240	66	-172	5
India	A5.IV.141	245	India	240	63	-172	250	62	-170	6
India	A5.IV.142	245	India	240	71	-174	250	71	-170	7
India	A5.IV.144	254	India	250	46	175	260	46	175	2

[a]Paleomagnetic poles from the appendix tables of Van der Voo (1993), used to determine the global APWPs. The paleomagnetic-pole positions are rotated into Eurasian coordinates. Pole numbers refer to the appendix table numbers 1,2,3,..., followed by the line number within the table, such that A1.033 is the 33rd pole in Table A1. Complete references are given by Van der Voo (1993). Rotation parameters are listed in Table 17.3.

[b]Van der Voo (1993) listed high and low ages for each pole; these are the averages of the high and low ages.

[c]Blocks are regions bounded by deformation, and the block names are different from the plate names. They are rotated independently (motions tabulated in Table 17.2).

Table 17.3. Rotation parameters for late Permian to early Cretaceous reconstructions in the weighted-global-mean frame of reference[a]

Block Name	Age	Pole Lat.	Pole Long.	Angle
N. America	130	69.16	112.92	53.81
N. America	140	64.66	108.52	55.86
N. America	150	73.27	100.02	57.16
N. America	160	78.95	89.57	62.48
N. America	170	74.18	68.33	67.10
N. America	180	73.52	48.63	69.79
N. America	190	72.47	36.90	70.88
N. America	200	71.33	39.17	71.20
N. America	210	67.54	45.10	71.38
N. America	220	65.53	56.29	70.83
N. America	230	63.59	64.92	70.63
N. America	240	61.16	73.94	70.71
N. America	250	58.62	75.36	71.05
N. America	260	53.50	76.80	72.09
Greenland	130	59.80	109.10	45.51
Greenland	140	54.84	106.96	48.25
Greenland	150	64.54	98.29	48.69
Greenland	160	71.56	90.04	53.47
Greenland	170	66.78	75.21	58.92
Greenland	180	66.89	59.74	61.77
Greenland	190	66.36	49.86	62.98
Greenland	200	65.06	51.33	63.49
Greenland	210	60.72	55.29	64.29
Greenland	220	58.07	64.46	64.07
Greenland	230	55.72	71.64	64.12
Greenland	240	52.96	79.28	64.48
Greenland	250	50.28	80.46	65.22
Greenland	260	44.98	81.64	67.12
Colorado Plateau	130	74.60	113.95	55.82
Colorado Plateau	140	70.09	107.87	57.44
Colorado Plateau	150	78.27	96.11	59.32
Colorado Plateau	160	83.01	76.76	65.03
Colorado Plateau	170	77.20	55.11	69.23
Colorado Plateau	180	75.26	34.13	71.98
Colorado Plateau	190	73.48	23.03	73.13
Colorado Plateau	200	72.53	26.14	73.34
Colorado Plateau	210	69.24	34.27	73.14
Colorado Plateau	220	67.98	46.87	72.28
Colorado Plateau	230	66.58	56.85	71.83
Colorado Plateau	240	64.62	67.40	71.65
Colorado Plateau	250	62.17	69.47	71.76
Colorado Plateau	260	57.10	71.82	72.32
S. America	130	77.45	146.98	43.26
S. America	140	73.73	129.82	42.52
S. America	150	84.09	142.35	42.31
S. America	160	84.38	-109.08	43.87
S. America	170	88.18	-22.22	42.24
S. America	180	81.82	-18.06	42.25
S. America	190	76.30	-17.30	42.63
S. America	200	76.75	-8.62	42.12
S. America	210	75.67	20.49	40.84
S. America	220	76.36	54.72	40.19
S. America	230	74.02	80.97	40.29
S. America	240	69.26	101.46	41.13
S. America	250	64.97	102.27	41.58
S. America	260	56.66	101.83	42.96
Arabia	130	-4.83	174.87	51.12
Patagonia	130	80.52	152.05	42.83
Patagonia	140	78.56	129.09	41.59
Patagonia	150	88.67	-176.24	42.03
Patagonia	160	81.09	-80.68	44.17
Patagonia	170	83.33	-40.96	42.35
Patagonia	180	77.29	-29.26	42.60
Patagonia	190	71.96	-25.32	43.19
Patagonia	200	72.65	-19.19	42.56
Patagonia	210	73.10	3.81	40.89
Patagonia	220	76.50	32.34	39.76
Patagonia	230	76.61	63.36	39.47
Patagonia	240	73.26	92.70	39.91
Patagonia	250	68.88	95.60	40.09
Patagonia	260	60.13	97.23	41.02
Eurasia	130	58.60	103.43	30.11
Eurasia	140	50.03	105.00	31.95
Eurasia	150	61.79	89.20	31.21
Eurasia	160	69.69	72.84	35.03
Eurasia	170	60.31	65.52	39.80
Eurasia	180	57.73	51.27	42.19
Eurasia	190	55.97	43.97	42.83
Eurasia	200	54.70	48.04	42.22
Eurasia	210	49.32	56.31	42.36
Eurasia	220	46.31	69.37	41.26
Eurasia	230	43.14	80.33	40.83
Eurasia	240	39.07	91.78	41.24
Eurasia	250	34.85	95.26	42.28
Eurasia	260	28.47	96.61	46.03
Iberia	130	10.51	161.43	29.66
Iberia	140	8.38	156.21	32.73
Iberia	150	14.52	160.11	24.89
Iberia	160	33.01	164.90	22.33
Iberia	170	41.88	141.12	24.41
Iberia	180	52.71	123.38	23.27
Iberia	190	57.67	106.87	22.55
Iberia	200	54.66	105.38	23.53
Iberia	210	44.98	103.10	26.30
Iberia	220	37.51	112.27	29.27
Iberia	230	32.33	118.47	32.22
Iberia	240	27.51	124.48	35.97
Iberia	250	24.59	123.68	38.36
Iberia	260	19.69	121.58	43.30
Svalbard Platform	130	61.13	102.69	31.56
Svalbard Platform	140	52.76	104.25	33.19
Svalbard Platform	150	64.07	87.99	32.71
Svalbard Platform	160	71.31	70.83	36.69
Svalbard Platform	170	62.03	63.76	41.27
Svalbard Platform	180	59.32	49.37	43.62
Svalbard Platform	190	57.53	42.05	44.24
Svalbard Platform	200	56.35	46.19	43.59
Svalbard Platform	210	51.19	54.67	43.57
Svalbard Platform	220	48.40	67.95	42.37
Svalbard Platform	230	45.39	79.10	41.83
Svalbard Platform	240	41.43	90.75	42.13
Svalbard Platform	250	37.24	94.29	43.05
Svalbard Platform	260	30.75	95.67	46.59
S. Africa	130	0.00	169.24	44.82
Tarim-Tian Shan	130	56.62	107.14	32.21
Tarim-Tian Shan	140	48.68	107.59	34.22
Tarim-Tian Shan	150	60.27	94.89	33.11
Tarim-Tian Shan	160	68.77	81.87	36.61
Tarim-Tian Shan	170	60.41	71.45	41.39
Tarim-Tian Shan	180	58.66	56.72	43.52
Tarim-Tian Shan	190	57.31	49.07	44.01
Tarim-Tian Shan	200	55.88	53.04	43.48
Tarim-Tian Shan	210	50.31	60.55	43.81
Tarim-Tian Shan	220	46.84	73.12	43.02
Tarim-Tian Shan	230	46.07	84.28	37.50
Tarim-Tian Shan	240	46.63	104.67	29.93
Tarim-Tian Shan	250	45.39	124.69	23.78
Tarim-Tian Shan	260	36.06	121.14	25.18
N. China Fold Zone	130	56.71	107.93	31.53
N. China Fold Zone	140	48.59	109.18	31.22
N. China Fold Zone	150	62.97	93.24	25.47
N. China Fold Zone	160	73.99	57.08	25.11
N. China Fold Zone	170	59.21	49.19	25.35
N. China Fold Zone	180	47.55	27.29	24.94
N. China Fold Zone	190	35.58	14.90	23.74
N. China Fold Zone	200	25.77	12.32	20.25
N. China Fold Zone	210	8.98	20.31	17.04
N. China Fold Zone	220	-12.96	29.14	11.40
N. China Fold Zone	230	-51.70	-48.98	12.42
N. China Fold Zone	240	-34.02	-89.77	29.52
N. China Fold Zone	250	-28.50	-92.40	48.40
N. China Fold Zone	260	-30.95	-99.36	45.07
N. China Block	130	58.00	105.22	28.21
N. China Block	140	49.00	107.54	27.80
N. China Block	150	64.60	85.36	22.38
N. China Block	160	72.96	36.53	22.65
N. China Block	170	56.36	38.97	23.01
N. China Block	180	41.99	20.19	23.46
N. China Block	190	28.61	9.33	23.13
N. China Block	200	17.56	6.38	20.19
N. China Block	210	-0.12	13.20	17.41
N. China Block	220	-24.47	17.27	12.41
N. China Block	230	-50.01	-52.23	15.83
N. China Block	240	-34.61	-86.80	32.72
N. China Block	250	-28.92	-90.24	51.46
N. China Block	260	-30.97	-97.50	53.81
India	130	-5.63	-163.38	97.19
India	140	-4.36	-164.00	98.56
India	150	-7.54	-158.79	93.45
India	160	-11.84	-152.92	89.44
India	170	-12.75	-154.60	85.94
India	180	-15.27	-154.14	82.31
India	190	-16.78	-153.96	78.81
India	200	-16.19	-155.11	78.85
India	210	-14.32	-158.77	78.94
India	220	-11.77	-160.87	82.75
India	230	-9.79	-162.20	86.39
India	240	-7.73	-163.29	90.94
India	250	-6.59	-164.93	92.10
India	260	-4.41	-168.30	94.12
E. Antarctica	130	-40.88	-92.46	15.97

Table 17.3. (contd.)

Block Name	Age	Pole Lat.	Pole Long.	Angle
Arabia	140	-4.20	171.37	54.65
Arabia	150	-5.32	175.58	47.98
Arabia	160	-6.45	-177.48	43.49
Arabia	170	-6.29	176.39	42.53
Arabia	180	-7.16	175.01	38.08
Arabia	190	-8.09	173.43	34.23
Arabia	200	-7.73	171.19	35.08
Arabia	210	-6.66	164.47	37.91
Arabia	220	-5.43	163.30	43.49
Arabia	230	-4.63	163.11	48.28
Arabia	240	-3.90	163.51	53.83
Arabia	250	-3.52	161.58	56.31
Arabia	260	-2.83	157.68	61.09
S. China	130	48.52	114.15	44.83
S. China	140	42.77	113.37	45.11
S. China	150	52.29	108.54	38.07
S. China	160	62.74	102.27	35.67
S. China	170	56.49	84.99	35.98
S. China	180	54.53	64.23	33.32
S. China	190	49.93	49.80	29.76
S. China	200	43.98	49.29	25.43
S. China	210	30.51	56.79	22.54
S. China	220	18.14	72.89	18.13
S. China	230	9.81	91.20	22.82
S. China	240	1.09	123.65	32.49
S. China	250	-3.30	138.75	47.45
S. China	260	-6.99	133.48	52.42
W. Africa	130	0.53	165.35	37.50
W. Africa	140	0.09	161.41	41.41
W. Africa	150	0.74	165.71	34.29
W. Africa	160	1.70	174.63	29.22
W. Africa	170	1.15	165.56	28.76
W. Africa	180	1.38	162.04	24.47
W. Africa	190	1.64	157.68	20.84
W. Africa	200	1.28	154.74	21.98
W. Africa	210	0.34	146.67	25.80
W. Africa	220	-0.12	147.80	31.47
W. Africa	230	-0.35	149.27	36.23
W. Africa	240	-0.52	151.26	41.66
W. Africa	250	-0.73	149.45	44.42
W. Africa	260	-1.11	145.74	49.80
Morocco	130	0.77	165.55	37.81
Morocco	140	0.35	161.62	41.73
Morocco	150	1.03	165.96	34.65
Morocco	160	2.00	174.85	29.64
Morocco	170	1.52	165.92	29.16
Morocco	180	1.83	162.56	24.88
Morocco	190	2.16	158.39	21.23
Morocco	200	1.80	155.45	22.35
Morocco	210	0.84	147.38	26.13
Morocco	220	0.32	148.35	31.80
Morocco	230	0.05	149.71	36.57
Morocco	240	-0.15	151.62	42.01
Morocco	250	-0.37	149.79	44.76
Morocco	260	-0.76	146.06	50.12

Block Name	Age	Pole Lat.	Pole Long.	Angle
S. Africa	140	0.00	165.57	48.56
S. Africa	150	0.00	169.82	41.63
S. Africa	160	0.00	177.50	36.82
S. Africa	170	0.00	170.28	36.10
S. Africa	180	0.00	168.15	31.69
S. Africa	190	0.00	165.65	27.89
S. Africa	200	0.00	163.12	28.87
S. Africa	210	0.00	155.78	32.18
S. Africa	220	0.00	155.37	37.87
S. Africa	230	0.00	155.78	42.70
S. Africa	240	0.00	156.79	48.24
S. Africa	250	0.00	154.89	50.87
S. Africa	260	0.00	151.06	55.96
NE. Africa	130	-2.21	167.26	43.60
NE. Africa	140	-2.14	163.72	47.46
NE. Africa	150	-2.31	167.64	40.39
NE. Africa	160	-2.42	175.21	35.32
NE. Africa	170	-2.53	167.66	34.85
NE. Africa	180	-2.79	164.96	30.52
NE. Africa	190	-3.07	161.83	26.83
NE. Africa	200	-3.01	159.37	27.90
NE. Africa	210	-2.83	152.31	31.48
NE. Africa	220	-2.56	152.54	37.18
NE. Africa	230	-2.37	153.37	41.99
NE. Africa	240	-2.21	154.76	47.48
NE. Africa	250	-2.15	152.99	50.18
NE. Africa	260	-2.06	149.37	55.42
E. Africa	130	-3.18	166.57	43.13
E. Africa	140	-3.07	163.08	47.03
E. Africa	150	-3.34	166.87	39.92
E. Africa	160	-3.53	174.40	34.76
E. Africa	170	-3.68	166.72	34.38
E. Africa	180	-4.07	163.80	30.09
E. Africa	190	-4.49	160.41	26.44
E. Africa	200	-4.39	157.98	27.55
E. Africa	210	-4.10	151.05	31.23
E. Africa	220	-3.68	151.52	36.92
E. Africa	230	-3.41	152.51	41.71
E. Africa	240	-3.16	154.05	47.18
E. Africa	250	-3.08	152.33	49.90
E. Africa	260	-2.94	148.78	55.19
Australia	130	-17.84	-132.21	40.21
Australia	140	-15.93	-135.51	40.28
Australia	150	-16.52	-119.76	40.19
Australia	160	-16.93	-104.45	43.76
Australia	170	-21.54	-102.35	41.38
Australia	180	-25.43	-95.98	41.77
Australia	190	-28.13	-90.44	41.40
Australia	200	-29.07	-91.98	40.31
Australia	210	-32.51	-97.40	36.97
Australia	220	-30.97	-107.77	35.82
Australia	230	-28.38	-116.33	35.84
Australia	240	-24.34	-125.03	36.95
Australia	250	-24.29	-130.32	36.51
Australia	260	-24.36	-141.14	35.97

Block Name	Age	Pole Lat.	Pole Long.	Angle
E. Antarctica	140	-41.76	-103.41	14.70
E. Antarctica	150	-23.17	-71.43	19.20
E. Antarctica	160	-12.29	-59.72	28.31
E. Antarctica	170	-17.60	-52.36	28.52
E. Antarctica	180	-19.11	-46.15	32.37
E. Antarctica	190	-19.65	-40.61	34.98
E. Antarctica	200	-21.24	-39.85	33.78
E. Antarctica	210	-27.18	-36.42	30.29
E. Antarctica	220	-32.31	-40.75	25.48
E. Antarctica	230	-37.28	-47.73	21.76
E. Antarctica	240	-42.95	-62.37	18.21
E. Antarctica	250	-51.13	-67.21	16.69
E. Antarctica	260	-70.75	-87.30	15.27
Madagascar	130	-2.43	172.27	40.51
Madagascar	140	-1.12	170.84	42.65
Madagascar	150	0.11	-178.91	34.80
Madagascar	160	-0.30	-161.99	28.62
Madagascar	170	-3.34	-165.93	24.92
Madagascar	180	-8.34	-161.74	20.63
Madagascar	190	-11.88	-159.15	16.88
Madagascar	200	-12.00	-164.57	17.09
Madagascar	210	-11.98	179.18	18.46
Madagascar	220	-8.55	173.49	23.64
Madagascar	230	-6.44	171.34	28.29
Madagascar	240	-4.60	170.48	33.78
Madagascar	250	-4.38	167.05	36.06
Madagascar	260	-4.14	160.69	40.59

[a]Rotation parameters used to rotate the paleomagnetic data are deriveable from this table simply by subtracting the Eurasian rotation from that of any other plate. Note that the Colorado Plateau rotation relative to North America is from Bryan and Gordon (1988); all other poles are based on the work of Rowley (1995).

Table 17.4. Mean poles (20 m.y. sliding window) by continent, summed globally at 10 m.y. intervals based on the poles in Table 17.2.

	Interval Age	Average Pole Age	N	kappa	A95	Mean Lat.[a]	Mean Long.	Rotated Lat. based on Global Mean	Rotated Long. based on Global Mean	Angular Distance from Global Mean
Weighted Global Mean	**130**	**126.4**	**5**	**165**	**6**	**76**	**-174**	**90**	**110**	**0**
Unweighted Continental Mean	130	126.8	4	49	13	80	148	81	50	9
N. America	130	125.4	5	112	7	73	-154	84	-102	6
Eurasia	130	128	1	150	8	76	155	83	80	8
Africa	130	126	4	80	10	80	177	86	28	4
S. America	130	128	4	98	9	73	177	86	139	4
Weighted Global Mean	**140**	**139**	**4**	**136**	**8**	**71**	**-178**	**90**	**105**	**0**
Unweighted Continental Mean	140	139	4	136	8	71	-178	90	92	0
Global Study Mean	140	140.7	7	82	7	69	-178	88	178	2
N. America	140	142	3	65	16	65	178	83	166	7
Eurasia	140	145	2	93	6	71	-167	86	-92	4
Africa	140	130	1	40	3	80	-179	81	3	9
S. America	140	139	1	50	11	69	176	87	136	3
Weighted Global Mean	**150**	**153.4**	**5**	**34**	**13**	**77**	**154**	**90**	**63**	**0**
Unweighted Continental Mean	150	153.6	5	34	13	77	154	90	63	0
Global Study Mean	150	152.3	14	23	8	74	161	87	-170	3
N. America	150	149.3	3	71	15	66	166	79	-180	11
Eurasia	150	149	4	50	13	70	-178	80	-142	11
Africa	150	155.5	2	5	25	74	155	88	164	2
S. America	150	158	1	18	9	73	135	84	88	6
E. Antarctica	150	156	3	196	9	78	29	68	0	22
Weighted Global Mean	**160**	**160.2**	**6**	**64**	**9**	**78**	**140**	**90**	**72**	**0**
Unweighted Continental Mean	160	160.7	5	73	9	76	142	88	151	2
Global Study Mean	160	159.8	20	32	6	75	143	87	158	3
N. America	160	162.8	4	71	11	69	128	81	111	9
Eurasia	160	158	4	48	13	72	173	80	-150	10
Africa	160	161.2	5	19	18	72	138	84	135	6
S. America	160	162	2	553	3	73	139	85	135	5
E. Antarctica	160	159.4	5	104	8	88	70	79	-29	12
Weighted Global Mean	**170**	**169.6**	**8**	**159**	**4**	**71**	**138**	**90**	**53**	**0**
Unweighted Continental Mean	170	169.8	6	165	5	72	140	89	-71	1
Global Study Mean	170	170	19	50	5	71	138	90	123	0
N. America	170	171.4	5	103	8	67	120	82	70	8
Eurasia	170	169	4	34	16	71	138	90	120	0
Africa	170	168.2	5	47	11	67	148	85	-175	5
S. America	170	166	1	10	6	72	138	90	-42	0
India	170	175	1	9	8	73	152	86	-103	5
E. Antarctica	170	169.3	3	70	15	80	157	80	-59	10
Weighted Global Mean	**180**	**178.8**	**6**	**237**	**4**	**67**	**124**	**90**	**42**	**0**
Unweighted Continental Mean	180	178.6	5	194	6	68	125	90	-83	0
Global Study Mean	180	179.8	17	56	5	66	125	89	130	1
N. America	180	182.3	3	152	10	65	117	86	62	4
Eurasia	180	175	2	7079	3	63	119	85	92	5
Africa	180	181.6	9	35	9	66	122	88	89	2
India	180	175	1	9	8	71	148	81	-114	9
E. Antarctica	180	179	1	245	3	71	124	86	-54	4
Weighted Global Mean	**190**	**192.1**	**9**	**132**	**5**	**65**	**110**	**90**	**21**	**0**
Unweighted Continental Mean	190	193.6	5	77	9	66	109	89	-46	2
Global Study Mean	190	191.7	29	91	3	66	113	89	-119	1
N. America	190	194	11	179	3	61	114	86	137	5
Eurasia	190	192.5	2	178	4	76	118	79	-80	11
Africa	190	187.5	11	101	5	65	109	89	-35	0
S. America	190	199	1	246	5	54	103	79	86	11
E. Antarctica	190	195	3	132	11	74	103	81	-58	10

Table 17.4. (contd.)

	Interval Age	Average PoleAge	N	kappa	A95	Mean Lat.[a]	Mean Long.	Rotated Lat. based on Global Mean	Rotated Long. based on Global Mean	Angular Distance from Global Mean
Weighted Global Mean	**200**	**196**	**8**	**128**	**5**	**64**	**112**	**90**	**29**	**0**
Unweighted Continental Mean	200	196.4	5	87	8	66	112	88	-68	2
Global Study Mean	200	196.4	27	73	3	64	113	89	154	0
N. America	200	196.7	14	105	4	60	114	86	122	4
Eurasia	200	192.5	2	178	4	76	118	79	-75	11
Africa	200	196.2	5	83	9	64	109	89	40	2
S. America	200	201.5	2	78	7	57	115	82	123	8
E. Antarctica	200	195	3	132	11	75	105	80	-56	11
Weighted Global Mean	**210**	**210.7**	**7**	**84**	**7**	**59**	**123**	**90**	**38**	**0**
Unweighted Continental Mean	210	211.2	5	69	9	59	128	88	-132	2
Global Study Mean	210	211.6	19	35	6	58	121	88	81	2
N. America	210	210.4	12	50	6	57	114	85	48	6
Eurasia	210	218.3	3	25	25	47	133	77	154	13
Africa	210	212.5	2	18	14	63	133	84	-99	6
S. America	210	204	1	0	13	58	128	87	-168	3
India	210	211	1	33	5	71	131	78	-68	13
Weighted Global Mean	**220**	**217.4**	**7**	**52**	**8**	**59**	**132**	**90**	**36**	**0**
Unweighted Continental Mean	220	217.9	5	43	12	60	137	87	-108	3
Global Study Mean	220	218.4	20	35	6	56	128	87	92	3
N. America	220	217.7	12	48	6	55	121	83	72	7
Eurasia	220	218.3	3	25	25	47	133	78	136	12
Africa	220	219	1	8	12	65	166	73	-104	17
S. America	220	223.7	3	59	16	60	139	87	-124	4
India	220	211	1	33	5	72	133	77	-50	13
Weighted Global Mean	**230**	**232.1**	**7**	**49**	**9**	**58**	**147**	**90**	**72**	**0**
Unweighted Continental Mean	230	233.4	5	38	13	60	150	88	-84	2
Global Study Mean	230	230.9	18	47	5	55	143	86	111	4
N. America	230	230	9	111	5	51	136	80	105	10
Eurasia	230	237	2	584	14	49	150	80	158	10
Africa	230	235	1	20	8	71	148	78	-35	12
S. America	230	228	5	42	12	59	143	88	52	2
India	230	237	1	43	5	66	-175	71	-85	19
Weighted Global Mean	**240**	**239**	**9**	**73**	**6**	**57**	**152**	**90**	**70**	**0**
Unweighted Continental Mean	240	238.5	5	49	11	61	155	86	-51	4
Global Study Mean	240	240	32	56	3	55	152	88	152	2
N. America	240	239.2	12	153	4	53	146	85	110	5
Eurasia	240	241.4	14	99	4	52	151	85	149	5
Africa	240	235	1	20	8	71	151	76	-28	14
S. America	240	234.5	2	17	14	57	148	88	68	2
India	240	242.3	3	321	7	67	-172	71	-74	19
Weighted Global Mean	**250**	**246.8**	**8**	**61**	**7**	**57**	**155**	**90**	**72**	**0**
Unweighted Continental Mean	250	248.8	4	32	17	61	156	86	-33	4
Global Study Mean	250	246.1	31	58	3	54	156	88	165	3
N. America	250	245.5	10	181	4	54	154	87	145	3
Eurasia	250	245.5	17	82	4	52	154	85	147	5
S. America	250	256	1	0	14	72	120	69	4	21
India	250	248	3	36	21	60	-177	75	-90	15
Weighted Global Mean	**260**	**255.8**	**6**	**69**	**8**	**52**	**163**	**90**	**70**	**0**
Unweighted Continental Mean	260	256.5	4	55	13	54	162	88	12	2
Global Study Mean	260	257.2	15	51	5	54	158	86	38	4
N. America	260	253	3	1294	3	52	162	89	73	0
Eurasia	260	256.3	7	105	6	49	157	85	108	5
S. America	260	262.8	4	57	12	65	146	74	10	16
India	260	254	1	411	2	46	175	81	-138	9

[a]All poles listed in Eurasian coordinates.

Table 17.5. Summary of pole statistics by study and by interval means by continent and global mean.

Component	N	Average A95 of the studies	N	Average A95 by interval mean
Weighted Global Mean			95	7.1
Unweighted Global Mean			67	10.4
Global Study Mean	147	6.6	268	5
N. America	55	6.2	106	7.3
Eurasia	35	5.5	67	10.9
Africa	25	9	47	10.9
S. America	17	9.1	28	10.1
India	6	5.5	12	7.6
E. Antarctica	9	5	18	9.3